J. Fluid Mech. (1991), *vol.* 222, *pp.* 61–94
Printed in Great Britain

Lyapunov exponents and the dimension of periodic incompressible Navier–Stokes flows: numerical measurements

By ROLAND GRAPPIN AND JACQUES LÉORAT
Observatoire de Meudon, F-92190 Meudon, France

(Received 28 February 1989 and in revised form 25 May 1990)

In this paper we study the quasi-stationary turbulent state developed by an incompressible flow submitted to a constant periodic force. The turbulent state is described by its Lyapunov exponents and Lyapunov dimension. Our aim is to investigate in particular if the dimension is, as several lines of argument seem to indicate, given in one way or another by the number of 'turbulent' modes present in the flow.

The exponents may be viewed as the asymptotic limits of local exponents, which are the divergence rates between the actual state of the fluid and nearby states. These local exponents fluctuate as the fluid suffers chaotic changes: they are systematically larger during bursts of excitation at large scale. In one case, we find that the flow oscillates repeatedly, on a very long timescale, between two distinct turbulent states, which have distinct local Lyapunov spectra and also distinct energy spectra. At the moderate resolutions studied here (64^2, 128^2 and 16^3), we find that the dimension of the attractor in flows with standard dissipation is bounded above by the number of degrees of freedom contained in the large scales, i.e. at wavenumbers smaller than that of the injection wavenumber k_f. We also consider two-dimensional flows with artificial terms (hyperviscosity), which concentrate small-scale dissipation in a narrow band of wavenumbers, and allow the formation of an inertial range. The dimension in these flows is no longer bounded by the number of large scales; it grows with, but remains significantly smaller than, the number of modes contained in the inertial range. It is conjectured that this is due to the presence of coherent structures in the flow, and that at higher resolutions also, the presence of coherent structures in turbulent flows will lead to an effective attractor dimension significantly lower than the estimations based on self-similar Kolmogorov theories.

1. Introduction

Simulating real, atmospheric or astrophysical flows is out of reach for now and the near future, owing to computer resources that are limited in time and memory. In practice, one has to model the flow in one way or another. Direct numerical simulations with pseudo-spectral methods are an example of 'minimal' modelling: they amount to computing the solutions of a subset of modes of the Navier–Stokes equations, keeping enough modes in this subset to represent both all the 'inertial' modes (those for which the nonlinear interactions dominate dissipative terms) and a reasonable number of the rest of them, the 'dissipative' modes.

If one could show that the dimension of the turbulent attractor of a given flow is much smaller than the number of modes necessary for a standard numerical

simulation, then it would be legitimate to look for a more economical tool than the Fourier basis (see for instance Kraichnan 1987). On the other hand, if the dimension is low, the associated chaos will probably be similar to the 'deterministic' chaos of other low-dimensional systems, while a large dimension would imply that a description is possible only in a statistical sense (Atten *et al.* 1984).

This question has received so far two kinds of contradictory answers:

(*a*) Analytical arguments by Constantin *et al.* (1985), as well as numerical computations of the Lyapunov dimension in models of fully developed turbulence (Grappin, Léorat & Pouquet 1986; Yamada & Ohkitani 1988; see also Manneville 1985) have given consistency to the idea that the number of degrees of freedom in fully developed turbulence grows as the number of modes contained in the inertial range (Landau & Lifshitz 1971). This seems to leave no hope for any substantial reduction of the number of degrees of freedom in turbulence modelling.

(*b*) On the other hand, direct measurements of the attractor dimension via numerical simulations of two-dimensional, incompressible, periodic flow, have given surprisingly low values. Using two different methods of calculations, Lafon (1985) and Grappin & Léorat (1987) reported values always below 25, for flows of resolution 64^2 and 128^2, which thus contained a total number of degrees of freedom about 2000 and 10^4 respectively.

We report in this paper a systematic study of periodic incompressible flows driven by a constant periodic force; a first account of the results was given in Grappin & Léorat (1987) (herein after referred to as GL87), and a preliminary version of this paper was published in Grappin & Léorat (1989). A periodic flow is an idealization of an homogeneous flow, and leads to the minimum computational constraint. The maximum resolution that we shall consider is 128^2 in two-dimensional flows, and 16^3 in three-dimensional flows. In two-dimensional flows, we found it interesting to compare flows with standard dissipation and artificial dissipation, the latter allowing a wider range of excited scales at a given resolution.

The main difference between two- and three-dimensional flows is that in the latter case, the direct transfer of excitation towards small sales is not inhibited by the (inviscid) conservation of enstrophy which holds in two-dimensional flows. Thus, larger dimensions might be obtained more easily in three-dimensional flows, at the price of still larger memory requirements for a given resolution, i.e. for a given ratio of the largest/smallest scale.

We write the two-dimensional incompressible Navier–Stokes equations in terms of the stream function ψ (the velocity being $\boldsymbol{u} = (\partial\psi/\partial y, -\partial\psi/\partial x)$) as

$$\frac{\partial\psi}{\partial t} + u^j\left(\frac{\partial\psi}{\partial x^j}\right) = F + \mathrm{D}(\psi), \tag{1a}$$

where F is the force, and D is the operator associated with dissipation. We shall use both the standard form:

$$\mathrm{D}(\psi) = \nu\nabla^2\psi, \tag{1b}$$

and another, less standard form, which combines two artificial dissipative terms, a hyperviscosity (iterated Laplacian) and a large-scale 'friction' (inverse Laplacian $\nabla^{-2}\psi$):

$$\mathrm{D}(\psi) = (-1)^{p-1}\nu_p\nabla^{2p}\psi + \nabla^{-2}\psi. \tag{1c}$$

The hyperviscosity term reduces to the standard Laplacian term when $p = 1$. $p > 1$ has been used to obtain a clearer separation of the dissipative scales from the inertial range (see Basdevant *et al.* 1981); it has been shown to provide results comparable

with those obtained at larger resolutions with $p = 1$, so long as some care is taken to keep a minimum number of dissipative scales. The friction term provides a large-scale sink for the energy that is transferred from smaller scales, hence it helps to establish more quickly a statistical equilibrium (see Babiano *et al.* 1987; Legras, Santangelo & Benzi 1988).

In two-dimensional flows, we consider two kinds of forcing: either a (constant) white noise in a definite frequency band, or a harmonic force with wavenumber k_f:

$$F(x, y) = f\cos(k_f y). \tag{1d}$$

In three-dimensional flows, we shall again consider either a white noise, or a small (ϵ) perturbation of the above harmonic force:

$$\boldsymbol{F} = (f\cos(k_f y), \epsilon\cos(\tfrac{1}{2}k_f x), \epsilon\cos(\tfrac{1}{2}k_f y)). \tag{1e}$$

One way to obtain a turbulent state is to start with an (unstable) equilibrium flow: a small perturbation will grow first linearly and then eventually generate chaos by nonlinear interactions. In two-dimensional flows, the so-called Kolmogorov flow (Kolmogorov 1960; Obukhov 1983) has the required properties; it is obtained by balancing the dissipation term $\mathrm{D}(\psi)$ with harmonic forcing in the x-direction ($1d$), so that $\mathrm{D}(\psi) = -F$. With standard dissipation ($1b$), it has the solution

$$\psi^0(x, y) = F(x, y)/(\nu k_f^2) = (f/\nu k_f^2)\cos(k_f y), \tag{2a}$$

so that the velocity is parallel to the x-direction, with its x-component given by

$$u_x^0 = -f/(\nu k_f)\sin(k_f y). \tag{2b}$$

Note that the nonlinear terms are zero. We define the initial Reynolds number as $R^0 \equiv u^0/(\nu k_f) = f/(\nu k_f)^2$. When $R^0 > \sqrt{2}$, this flow is linearly unstable, in particular to large-scale perturbations in the y-direction (at $k = \frac{1}{2}k_f$ when R^0 is large enough; see Meshalkin & Sinaï 1961, Green 1974; also Grappin, Léorat & Londrillo 1988).

With the artificial dissipation term ($1c$), the friction term $\nabla^{-2}\psi$ is dominant at large scale, so that the amplitude ψ^0 of the Kolmogorov flow is given $\nabla^{-2}\psi = -F$, or

$$\psi^0 = k_f^2 f\cos(k_f y), \tag{3a}$$

and the x-component of the velocity is

$$u_x^0 = -f k_f^3 \sin(k_f y). \tag{3b}$$

The criterion for the instability of the Kolmogorov flow now becomes $\tilde{R}^0 = u^0 k_f^3 = f k_f^6 > \sqrt{2}$.

The instability of the Kolmogorov flow may be used as a basic ingredient in scenarios for the transfer of excitation towards much larger scales ($k \ll k_f$) (Green 1974; She 1987). With one exception, the flows that we shall consider in this paper will show a large-scale transfer restricted to one or two octaves, as the initial characteristic scale will be one half or one quarter of the size of the periodic box: $k_f = 2$ or 4. In this case, the perpendicular instability of mode $\frac{1}{2}k_f$ in a Kolmogorov flow of wavenumber k_f directly drives the onset of turbulence in two-dimensional flows (see for instance Grappin *et al.* 1988).

A three-dimensional generalization of the Kolmogorov flow is provided by the so-called ABC flows, which are generally unstable above a critical Reynolds number, with a growth time comparable with the dynamical timescale of the flow when the Reynolds number is large enough (Galloway & Frisch 1987). We shall not investigate such flows in detail. We shall obtain a three-dimensional turbulent state via either

a slight perturbation of the Kolmogorov forcing (1*e*), or via a white-noise forcing in a wavenumber band around k_f.

We now define some notation. In flows with standard dissipation (1*b*), we define the integral and Taylor Reynolds numbers as $R_i = U/\nu k_i$ and $R_\lambda = U/\nu k_\lambda$, where U is the r.m.s. velocity, and the wavenumbers are defined from the energy spectra E_k as

$$k_i = \int E_k \,\mathrm{d}k \Big/ \left\{ \int E_k \,\mathrm{d}k/k \right\} \quad \text{and} \quad k_\lambda = \left\{ \int k^2 E_k \,\mathrm{d}k \Big/ \int E_k \,\mathrm{d}k \right\}^{\frac{1}{2}}.$$

When starting the integration with a flow of well-defined amplitude u and wavenumber k_f, we shall also use the 'initial' Reynolds number $R^0 = u/(\nu k_f)$. When using a hyperviscosity ν_p, with $p > 1$, (1*c*), the standard definitions of Reynolds numbers cannot be used; we define a modified Reynolds number R_p as

$$R_p = U/(k_p^{2p-1} \nu_p), \tag{4a}$$

with

$$k_p = \left\{ \int k^{2p} E_k \,\mathrm{d}k \Big/ \int E_k \,\mathrm{d}k \right\}^{1/(2p)} \tag{4b}$$

so that when $p = 1$ one recovers the usual definition of the Taylor Reynolds number and wavenumber, $R_1 = R_\lambda$ and $k_1 = k_\lambda$.

The plan of the paper is as follows. Section 2 contains a description of the numerical method. Section 3 describes the onset of turbulence in two-dimensional flows with standard dissipation. In §4, we investigate the relation between the dimension and the parameters of the flow: we consider in turn two-dimensional flows with standard dissipation and artificial dissipation, and three-dimensional flows; finally we study the properties of the basis of Lyapunov vectors. Section 5 is a summary and conclusion.

2. Measuring the Lyapunov exponents of turbulent flows

In order to measure the dimension of the Navier–Stokes equations, we shall use the method described in GL87, which consists in computing Lyapunov exponents, from which the Lyapunov dimension may be deduced via the Kaplan–Yorke formula. We give here an account of the method and of the way we have applied it to the case of the two-dimensional Navier–Stokes equations (1); we shall mention the difference arising from an extension to the three-dimensional case.

To evaluate the first (largest) Lyapunov exponent, we need to integrate two equations in parallel: the Navier–Stokes equations (1) for the stream function ψ, and the equation for the linearized stream function $\delta\psi$, linearized about ψ:

$$\frac{\partial \delta\psi}{\partial t} + u^j \frac{\partial \delta\psi}{\partial x^j} + \delta u^j \frac{\partial \psi}{\partial x^j} = \mathrm{D}(\delta\psi), \tag{5}$$

with $\delta \boldsymbol{u} = (\partial\delta\psi/\partial y, -\partial\delta\psi/\partial x)$. Consider the norm $\epsilon(t) = \|\delta\psi(t)\|$. It is a linear measure of the distance between the actual state ψ of the fluid and a nearby state $\psi + \delta\psi$, and may be considered as the error in measuring the true state of the fluid, given an initial error $\epsilon(t^0)$. The asymptotic limit of the growth rate of this error ϵ defines the first Lyapunov exponent λ_1:

$$\lambda_1 = \operatorname*{Lim}_{t\to\infty} \frac{\log\{\epsilon(t)/\epsilon(t^0)\}}{(t-t^0)}. \tag{6}$$

Benettin *et al.* (1980) have shown how to obtain numerically the whole set of

Lyapunov exponents, corresponding to average error growth rates in the different (orthogonal) directions of phase space. The total number of exponents is equal to the total dimension N of the phase space of the numerical solution of (1), i.e. to the number of degrees of freedom present in the numerical system. Note however that in practice it will not be necessary to compute the whole spectrum of exponents, but only a limited number M (see below).

The procedure is as follows. We integrate (5) with M independent initial states $\delta\psi^{i0}$, the set $\{\delta\psi^{i0}\}$ being orthonormal. We re-orthonormalize, at regular time intervals, the set of M linear solutions $\delta\psi^i(t)$, using the Gram–Schmidt procedure. As a byproduct, we obtain the increase of the norms $\epsilon_i = \|\delta\psi^i(t)\|$ of the solutions in each orthogonal direction of phase space. We define now the 'local' Lyapunov exponents $\lambda_i(t)$ as the local growth rates of the errors $\epsilon_i = \|\delta\psi^i(t)\|$ measured in the finite time interval $[t^0, t]$:

$$\lambda_i(t) = \frac{\log\{\epsilon_i(t)/\epsilon_i(t^0)\}}{(t-t^0)}, \quad i = 1 \text{ to } M. \tag{7}$$

As in (6), the Lyapunov exponents λ_i are the asymptotic limit of the local exponents $\lambda_i(t)$ when $t \to \infty$.

In both (6) and (7), t^0 is the time at which we choose to start to evaluate the exponents; it is not necessarily equal to the time corresponding to the initial state of the fluid. Indeed, although the asymptotic limits λ_i are independent of t^0 (see Oseledec 1968), the transient behaviour will also be of interest, as we shall see that the dependence of the $\lambda_i(t)$ on t^0 at finite times t gives interesting information on the fluid behaviour.

To be able to orthonormalize, we have to define a scalar product on $\mathbb{R}^N$ (recall that N is the total number of degrees of freedom of the solution). N is actually smaller than the number of grid points in the periodic box, since we use a standard isotropic truncation of the set of Fourier modes, eliminating wavenumbers larger than $k_{\max}$, which is equal to half the number of grid points in each direction of our periodic box. Moreover, the two (or three) components of the velocity are not independent, owing to the incompressibility of the flow ($\operatorname{div} \boldsymbol{u} = 0$). This leaves about $N \approx \pi k_{\max}^2$ degrees of freedom in two-dimensional flows, and $N \approx \frac{8}{3}\pi k_{\max}^3$ in three-dimensional flows.

In the two-dimensional case, we define the scalar product of two solutions of (5), χ and ϕ, by the real part of the Hermitian product of their Fourier transforms $\hat{\chi}$ and $\hat{\phi}$: $\langle\psi, \phi\rangle = \sum \operatorname{Re}(\hat{\chi}_n, \hat{\phi}_n^*)$, where the summation is made on all modes n, such that $k_x \geqslant 0$, which are precisely those stored in the computer. This definition (which differs only slightly from the standard L^2 inner product) allows a fast numerical computation. One checks that it indeed satisfies the properties of a scalar product, which is all that is required for the exponents to converge (Oseledec 1968; Benettin *et al.* 1980).

In the three-dimensional case, we integrate all three components of the velocity. We start initially with a divergence-free field, impose a divergence-free external force, and check that the velocity field remains solenoidal. We define the scalar product as in the two-dimensional case, with the summation now made on the three components of the velocity Fourier modes. We have checked numerically that this definition leads to the correct Lyapunov dimension in both the two- and three-dimensional cases, and in particular that the Lyapunov dimension of inviscid flows is equal to (and not larger than) N (see (9) below).

There are as many Lyapunov exponents as there are independent degrees of freedom in the system (N). The dimension of the attractor is less than N: it is

obtained by noting how many exponents are necessary for the cumulated sum $\Lambda(n) = \lambda_1 + \lambda_2 + \ldots + l_n$ (with $\lambda_1 > \lambda_2 > \ldots > \lambda_M$) to change its sign. In other words, the integer part of the dimension N_c satisfies $\Lambda(N_c \geqslant 0$ and $\Lambda(N_c+1) < 0$. Kaplan & Yorke (1979) give the following interpolation formula for the Lyapunov dimension d_L:

$$d_L = N_c + \Lambda(N_c)/|\lambda_{N_{c+1}}|. \tag{8}$$

The sum of all Lyapunov exponents, $\Lambda(N)$, is the rate of contraction of an N-volume in phase space. It can be expressed in terms of the product of the viscosity ν by the sum of the squares of the wavenumbers k_n:

$$\Lambda(N) = -\nu \sum_{n=1}^{N} k_n^2. \tag{9}$$

This formula implies in particular that, when $\nu = 0$, $\Lambda(N) = 0$, i.e. $d_L = N$; more generally, (9) can provide a test for the numerical procedure when all N Lyapunov exponents are known ($M = N$).

Note that computing M exponents increases the time and memory needs by a factor $(M+1)$, compared to integrating the Navier–Stokes equations (1) alone. As seen from (8), the only constraint for M is that it has to be larger than the dimension d_L (if we calculate an insufficient number of exponents, we still would be able to find an estimation of d_L by extrapolating the curve $\Lambda(n)$ to guess its intersection with the origin; this procedure will not be used in this paper). The dimension is of course unknown when we begin the calculation, but an *a priori* upper estimation (based on preliminary runs) allows us to choose M. Typically, M will be between about 10 and 100, and N between about 3000 and 12000. To obtain stable temporal averages and a well-ordered Lyapunov spectrum (i.e. $\lambda_1 > \lambda_2 > \ldots > \lambda_M$) requires simulations over very long durations, typically 60000 time steps, or 1000 turnover times; we shall study the convergence problem in some detail, although we shall not feel obliged to meet stringent convergence criteria such as those developed for smaller systems (see Manneville 1985).

The computations have been done on a CRAY 2 which provides a multitasked system with four processors. Multitasking was used in the following way. We give to each of the four processors the task of computing independently the nonlinear solution ψ together with one quarter of the M linear solutions $\delta\psi^i$. The reason why each processor has to integrate its own version of (1) is because the new value of ψ is needed at each time step to proceed with the integration of each of the $\delta\psi$ trajectories, and we do not want the processors to wait for one another at each time step. About every 1000 to 4000 time steps, the whole set of linear solutions $\delta\psi_i$ is copied to the main processor, which orthonormalizes them. Such a procedure allows a high degree of multitasking, and proves to be a good choice even when computing a small set of exponents.

We use a spectral code with periodic boundary conditions, explicit time-stepping (Adams–Bashforth scheme) for nonlinear terms, and implicit Cranck–Nicolson scheme for dissipative terms. The two-dimensional code is the same as the one used in Grappin *et al.* (1988).

Table 1 gives a summary of the runs, with the measured Lyapunov dimension d_L, and the main parameter: ν is the viscosity, k_f the forcing wavenumber (the unit wavenumber is $k_0 = 2\pi L$, where L is the size of the periodic box); dt is the time step, T is the integration time, U, k_λ and $\tau_{NL} = (k_\lambda U)^{-1}$ are time-averaged quantities: r.m.s. velocity, Taylor wavenumber and nonlinear turnover time. There are three

Run	Res	ν	k_f	dt	T	U	k_λ	τ_{NL}	N	d_L
AX	64^2	0.12	4	0.002	160	1.22	3.30	0.25	3000	0
AZ	64^2	0.08	4	0.003	430	0.96	3.20	0.33	3000	6.3
AS	64^2	0.06	4	0.004	320	1.10	3.10	0.29	3000	13
AP	64^2	0.03	4	0.008	320	1.00	1.80	0.56	3000	8.6
AK	64^2	0.015	4	0.01	600	0.88	1.80	0.63	3000	17
AG	64^2	0.005	8–10	0.01	80	0.32	6.20	0.51	3000	123
AL	8^2	0	2	0.04	200	0.84	1.70	0.70	28	28
AN	16^2	0.01	2	0.02	200	0.47	1.30	1.64	148	8.5
AP1	32^2	0.005	4	0.01	200	0.51	1.50	1.31	708	29
Bbx	64^2	[0.3]	2	0.08	120	0.82	2.39	0.51	3000	0
Bzz	64^2	[0.06]	2	0.08	120	0.93	2.33	0.46	3000	5.4
Bcg	128^2	[0.16]	2	0.04	120	0.95	2.32	0.45	12452	5.5
Bcc	128^2	[0.03]	2	0.04	120	0.98	2.30	0.44	12452	12
Bzs	64^2	[0.3]	2	0.08	120	0.99	2.31	0.44	3000	21
Bbg	64^2	[0.16]	2	0.08	120	1.00	2.29	0.44	3000	27
Bbb	64^2	[0.08]	2	0.08	120	1.01	2.28	0.43	3000	30
Bze	64^2	[0.3]	2	0.08	120	1.02	2.26	0.43	3000	50
CY	16^3	0.01	2	0.02	240	0.29	2.48	1.38	2836	48
CE	16^3	0.01	2	0.02	160	0.29	2.61	1.30	2836	57
CJ	16^3	0.005	2	0.02	80	0.30	3.47	0.95	2836	105

TABLE 1. Summary of runs. The first letter of the run indicate the type of the run: A and B denote two-dimensional simulations, C denotes three-dimensional simulations. ν is viscosity, k_f is the injection wavenumber, dt is time step, T is the integration time. U, k_λ and τ_{NL} are time-averaged quantities: r.m.s. velocity, Taylor wavenumber and nonlinear turnover time $\tau_{NL} = 1/(k_\lambda U)$. N is the total number of degrees of freedom present in the simulation, and d_L the Lyapunov dimension measured at time T. In the case of runs with artificial dissipation (beginning with B), ν is an equivalent viscosity (see text).

types of runs, denoted by the first letter of the run: A (resp. B) denotes two-dimensional simulations with standard dissipation (1*b*) (resp. artificial dissipation (1*c*)); C denotes three-dimensional simulations. In the case of runs with artificial dissipation (type B), we do not specify the parameters p and ν_p (see below table 3), but indicate instead between brackets the 'equivalent' viscosity ν which, if put in front of a standard ($p = 1$) dissipation term, would lead to the same dissipation rate as the iterated Laplacian term (1*c*) at maximum wavenumber k_{max}: $\nu k_{max}^2 = \nu_p k_{max}^{2p}$.

3. The onset of turbulence in two-dimensional periodic flows

We consider in this section two-dimensional flows with standard dissipation (type A), and examine how the dimension and exponents converge, illustrating the evolution of the flow towards a turbulent attractor. We begin by giving a classical description (i.e. using energy spectra and related quantities) of the onset of chaos and of the quasi-stationary state which is established when forcing balances turbulent dissipation in the average.

In the turbulent phase, the maximum Reynolds number that we reach is about 80 (see table 2). Much larger Reynolds numbers, and much larger resolution, are necessary to obtain fully developed turbulence (see for instance Brachet *et al.* 1988; Legras *et al.* 1988). For the purpose of this study, it will be sufficient that the Reynolds number R^0 based on the amplitude of the equilibrium flow is clearly above the threshold value for nonlinear chaos (i.e. $\lambda_1 \geqslant 0$, or $d_L > 0$), which appears here to be between 4 and 6 in two-dimensional flows (see runs AX and AZ, in table 2).

Run	AX	AZ	AS	AP	AK	AG	AL	AN	AP1
Res	64^2	64^2	64^2	64^2	64^2	64^2	8^2	16^2	32^2
k_f	4	4	4	4	4	8, 10	2	2	4
ν	0.12	0.09	0.06	0.03	0.015	0.005	0	0.01	0.005
R^0	4.2	6.2	8.3	16.7	33.3	*	∞	55	74
dt	0.002	0.003	0.004	0.008	0.01	0.01	0.04	0.02	0.01
T	160	430	320	320	600	80	200	200	200
U	1.22	0.96	1.09	1	0.88	0.32	0.84	0.47	0.51
R_l	3.4	4.8	6.3	29	49	15	∞	38	81
R_λ	3.1	4.5	5.9	18.6	33	10	∞	37	67
k_λ	3.3	3.2	3.1	1.8	1.8	6.2	1.7	1.3	1.5
N	3000	3000	3000	3000	3000	3000	28	148	708
N_{LS}	48	48	48	48	48	310	12	12	50
d_L	0	6.3	13	8.6	17	123	28	8.5	29

TABLE 2. Two-dimensional runs (with standard dissipation). Res is the number of grid points, k_f the injection wavenumber, ν the viscosity, R^0 the initial Reynolds based on the amplitude of the initial (Kolmogorov) flow, dt is time step, T is integration time. U, R_l, R_λ and k_λ are time-averaged quantities. N is the total number of degrees of freedom, $N_{LS} = \pi k_f^2$ is the number of degrees of freedom with wavenumber smaller than k_f, d_L is the Lyapunov dimension computed in the time interval $[0, T]$.

Figures 1–5 illustrate the results obtained for the four main runs of type A that we shall analyse in some detail: AK, AP and AS (which are commented in this Section) and AG (which is commented in the next Section).

3.1. *General properties of the chaotic state*

If the initial Reynolds number is substantially larger than critical (R^0 must be larger than about 5, see table 2), turbulence sets in as soon as the unstable large scales have reached about unity. This turbulent state is characterized by slow fluctuations of x- and y-components of the energy, the frequency of the oscillations being near the value of the first Lyapunov exponent (Grappin *et al.* 1988). Note that above this threshold, the dimension does not grow monotonically when R^0 is increased (see table 2).

An important requirement, in measuring the attractor's dimension, is that the flow must have reached (statistical) stationarity. Let us examine in some detail three cases with growing viscosities: $\nu = 0.015$, 0.03 and 0.06 (runs AK, AP and AS respectively). The injection wavenumber is $k_f = 4$, the forcing amplitude is $f = \frac{1}{2}\nu k_f^2$, and the initial flow is a white-noise perturbation of the Kolmogorov flow (2), so that the amplitude of the unperturbed flow is the same for all three runs: $u^0 = \frac{1}{2}k_f = 2$ (hence the initial r.m.s. energy is $E^0 = 1$). The Reynolds numbers based on the amplitude of the flows are thus $R^0 = u/(\nu k_f = 1(2\nu)$, or 33.3, 16.7 and 8.3 respectively (see table 2).

Although the initial conditions are identical for all runs, the average properties of the turbulent state which establishes itself after the linearly unstable transient phase are different. We show in figure 1(*a–c*) the spectra of x-, y- and total energies, averaged over the time interval $[0, 300]$. Small scales ($k > k_f = 4$) appear to be isotropic, but not the large scales: the y-direction dominates in runs AK and AP, the x-direction dominates in run AS. (Note that in figure 1 and in the following, x-, y-components are denoted by continuous and dashed lines respectively, and the total component by dotted lines). The medium scales are Reynolds-number independent: the energy level at $k = 10$ is almost exactly identical in the three runs (dashed

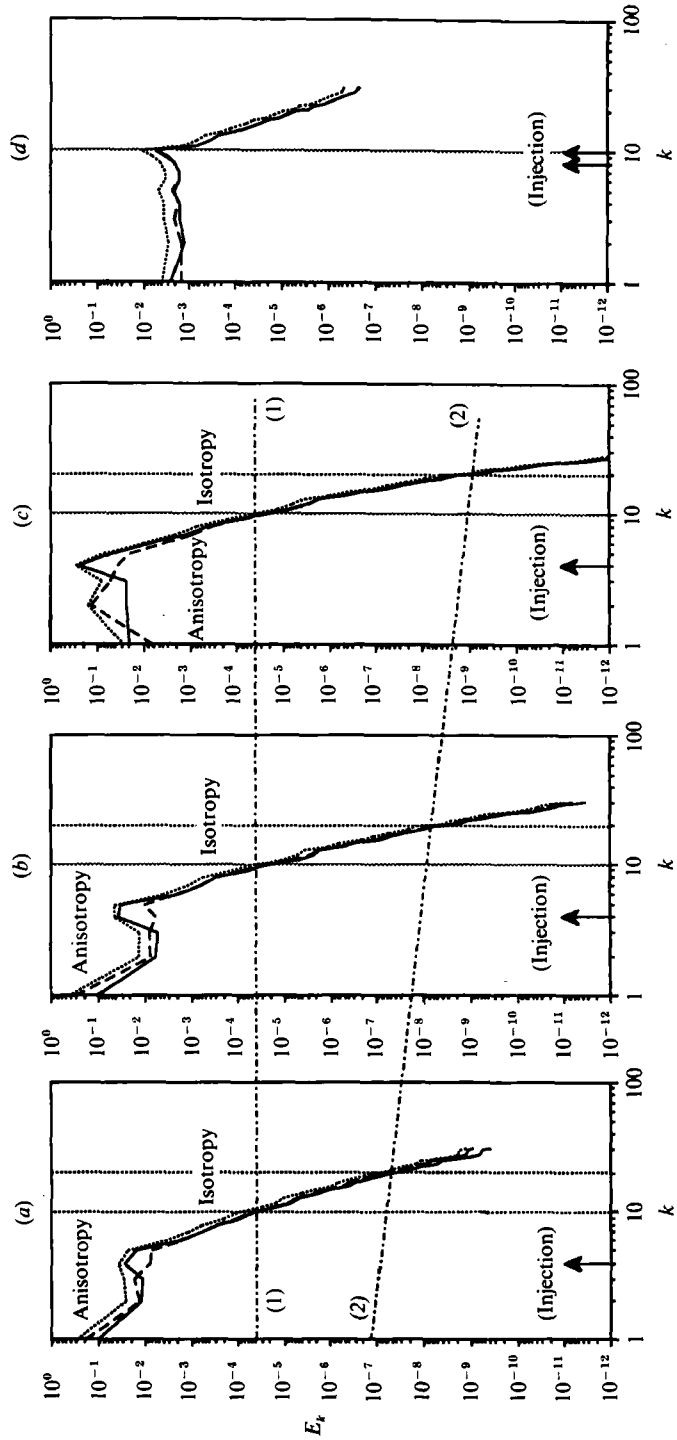

FIGURE 1. Time-averaged energy spectra E_k in two-dimensional flows (runs AK, AP, AS and AG at respective times $t = 600, 300, 300, 80$; see table 2). Continuous lines indicate the x-component, dashed lines the y-component, and dotted lines the total component. In the first three spectra, line (1) joins the spectra at wavenumber $k = 10$, line (2) joins the spectra at $k = 20$. (*a*) Run AK, (*b*) run AP, (*c*) run AS, (*d*) run AG.

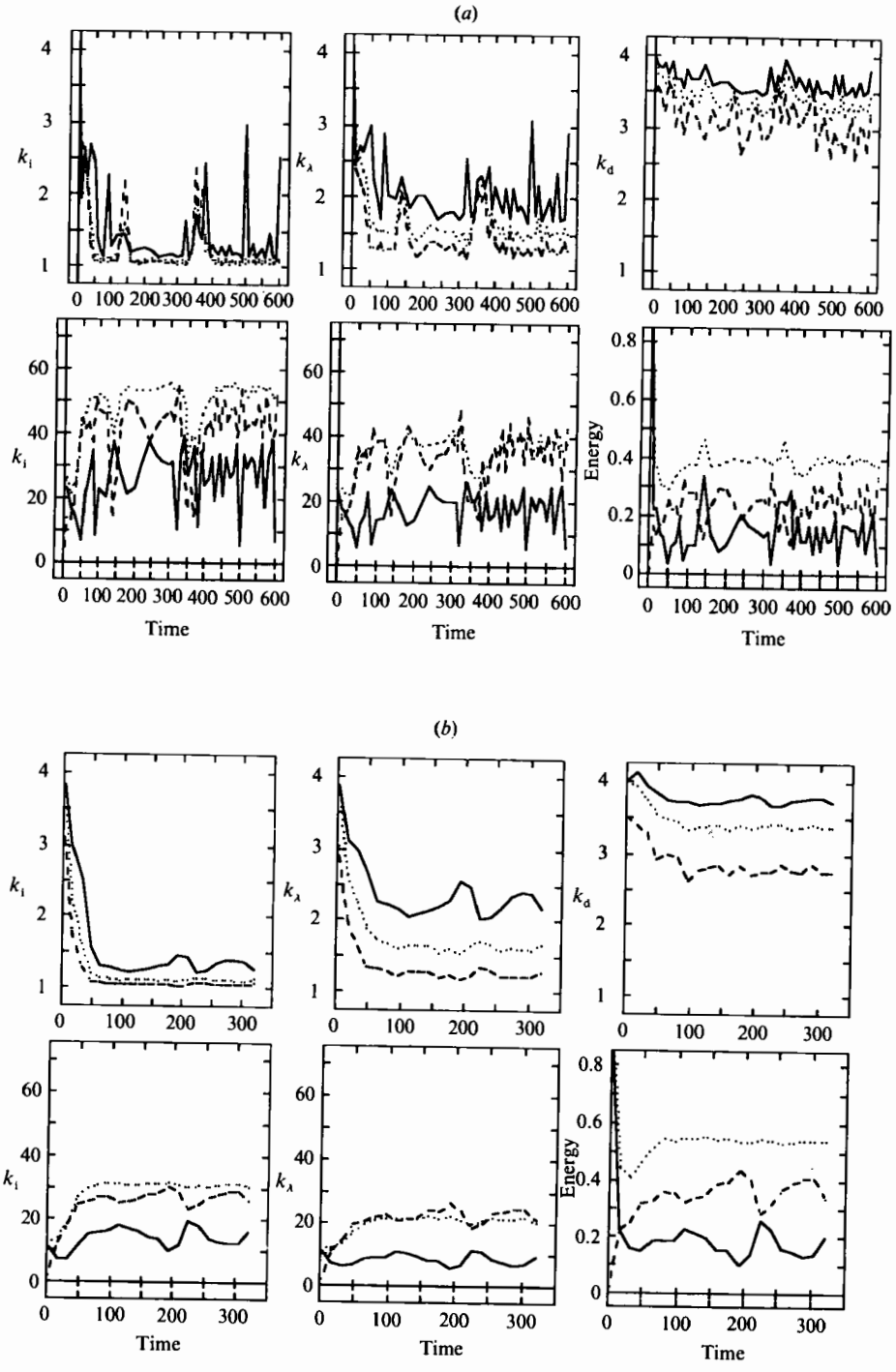

FIGURE 2(a,b). For caption see facing page.

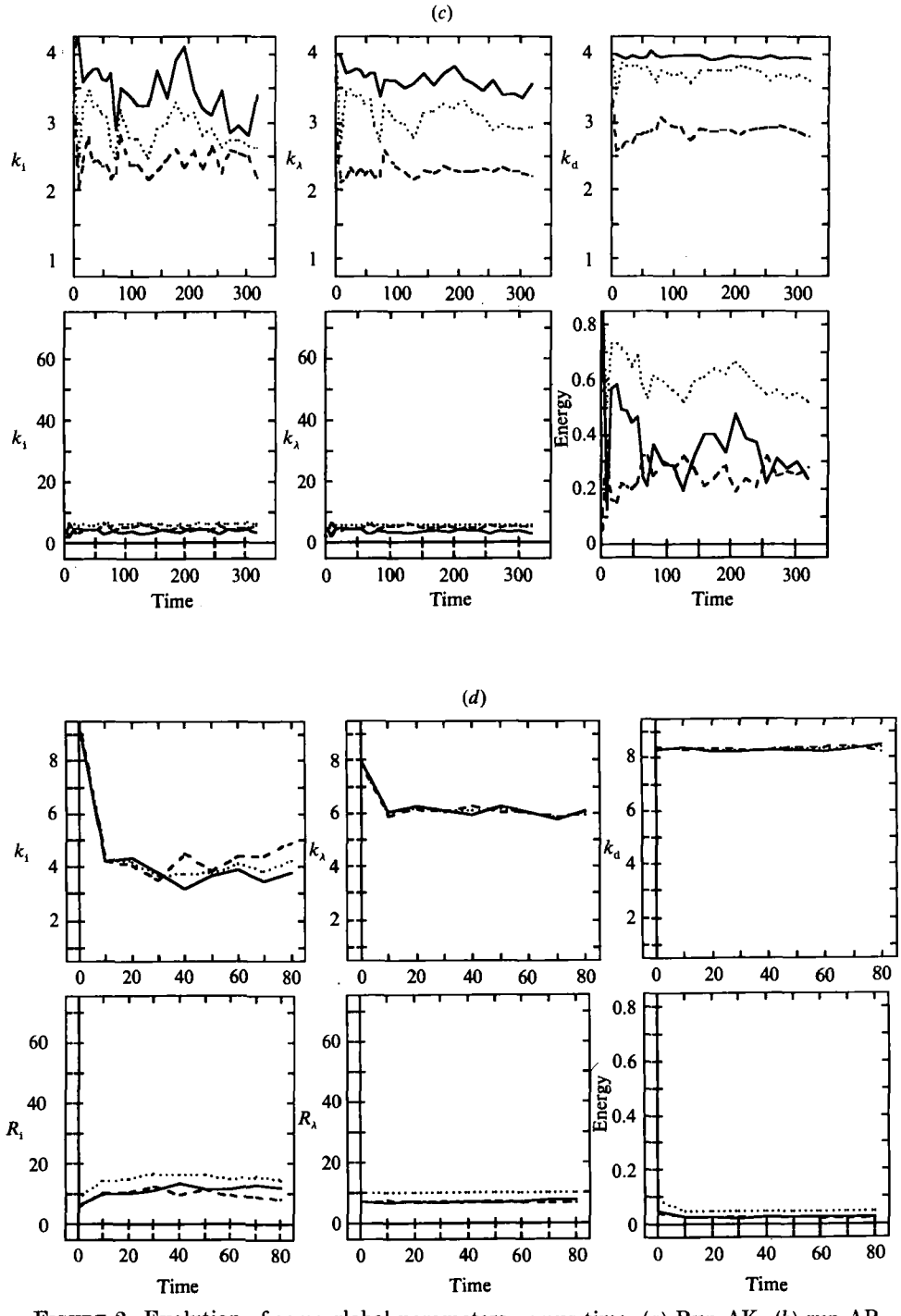

FIGURE 2. Evolution of some global parameters versus time. (*a*) Run AK, (*b*) run AP, (*c*) run AS, (*d*) run AG. Notation as in figure 1.

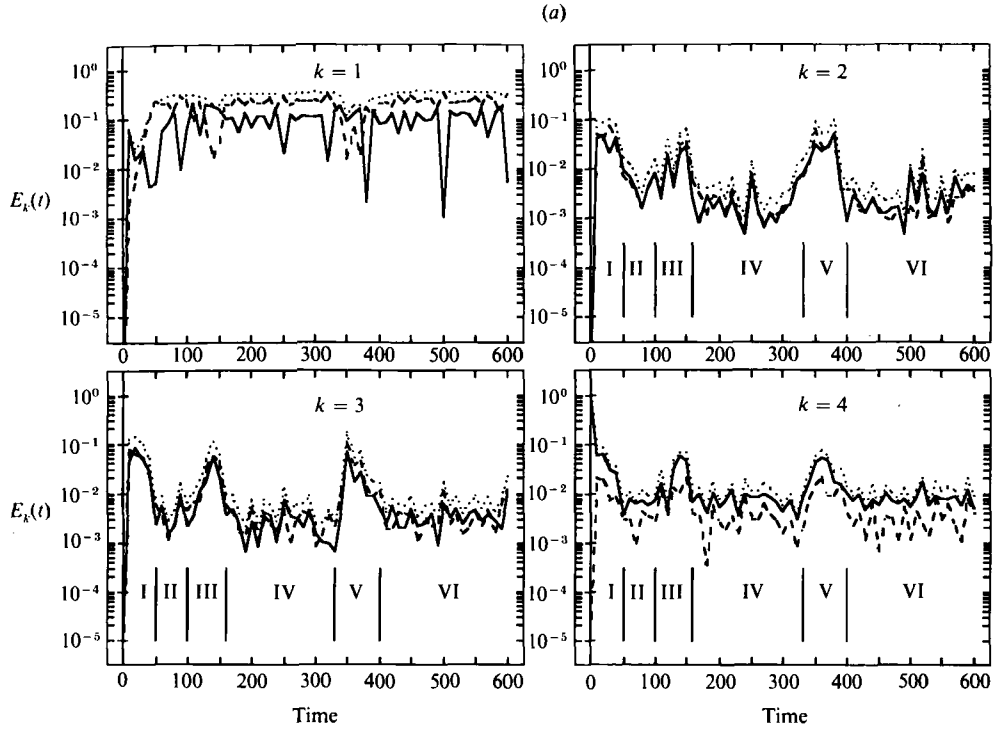

FIGURE 3(a,b). For caption see facing page.

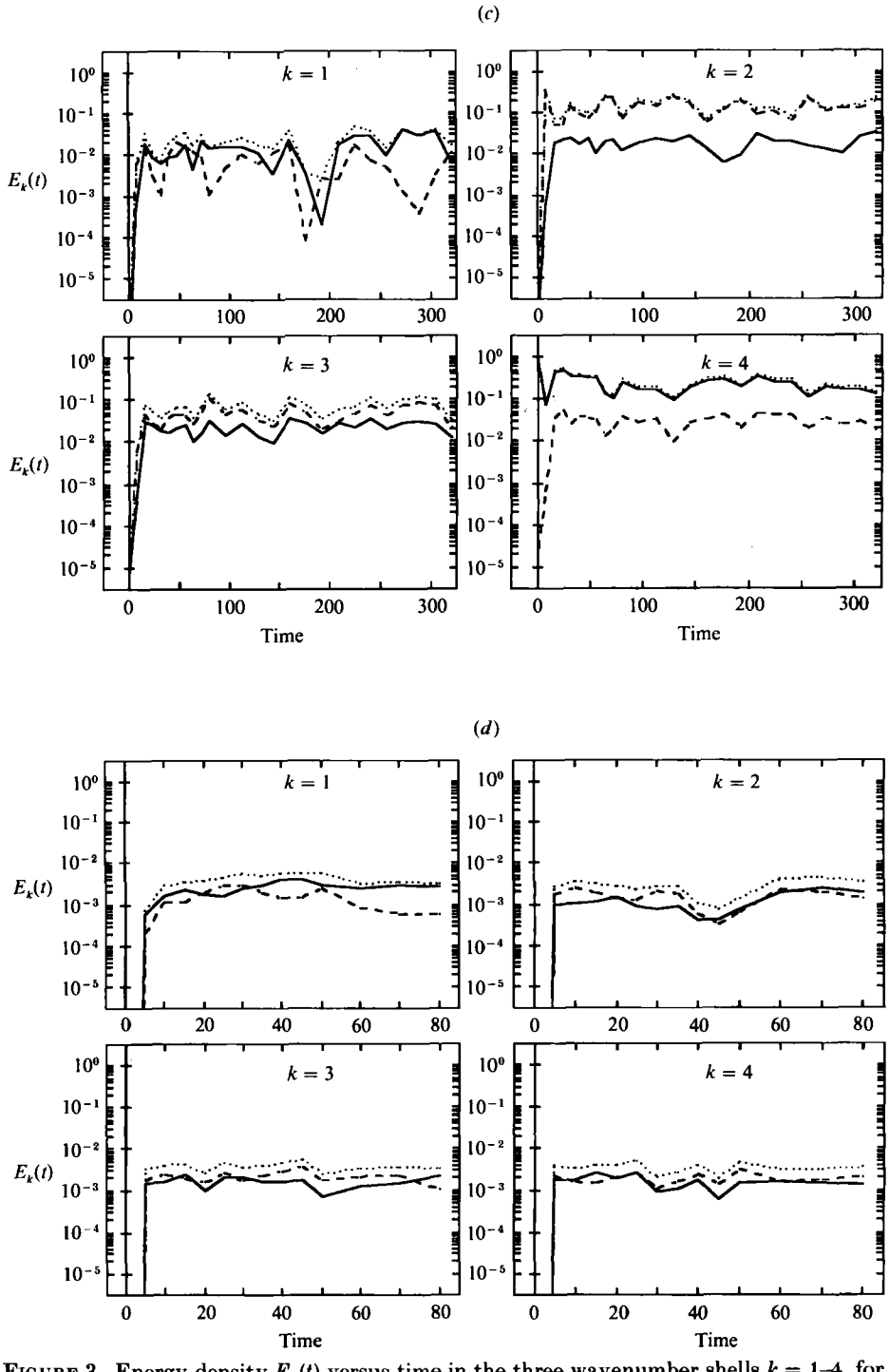

FIGURE 3. Energy density $E_k(t)$ versus time in the three wavenumber shells $k = 1$–4, for the x-, y- and total energies. (*a*) Run AK, (*b*) run AP, (*c*) run AS, (*d*) run AG. Notation as in figure 1. The roman numerals in (*a*) denote phases (see text, §3.2).

line (1) in the figure). Last, increasing the viscosity reduces the level of small-scale excitation, as expected (see the dashed line (2) which connects the energy levels at $k = 20$ in the figure).

Figure 2(*a–c*) shows the time evolution of some quantities: the integral, Taylor and dissipation wavenumbers k_i, k_λ, and k_d, the integral and Taylor Reynolds numbers R_i and R_λ. In the three runs, R_λ fluctuates respectively around 30, 20 and 5. The early quasi-linear large-scale instability results in an initial decrease of the integral wavenumber k_i, which drops from 4 down to about unity for run AK and AP and to about 3 for run AS. The energy E also decreases initially (in one turnover time): this is because the excitation is transferred towards smaller scales, which induces an increase in the total dissipation rate.

Figure 3(*a–c*) shows, for the three runs separately, the time evolution of the energies in each of the wavenumber shells $k = 1$ to 4, and allows an estimate of the actual fluctuations of the large-scale modes about the average level shown in figure 1.

3.2. *Do the local exponents and the dimension converge?*

In order to examine the convergence of λ_i and d_L, we found it convenient to plot the logarithm of the first ten errors $\epsilon_i(t)$ instead of $\lambda_i(t)$: figure 4(*a–c*) shows the $\epsilon_i(t)$, for $i = 1$ to 10, and for runs AK, AP and AS. Recall that the local exponent $\lambda_i(t)$ is but the average slope of $\log \epsilon_i(t)$ in the interval $[t^0, t]$ (equation (7)). Note that decreasing the viscosity does not systematically increase the number of positive exponents: it is smallest for run AP, which has the intermediate viscosity and Reynolds numbers; note also that the smallest amplitude of the fluctuations occurs for the intermediate viscosity and Reynolds number (run AP, see figure 3*b*).

One sees that, except for run AS (with lowest R^0), the local exponents are far from constant. In particular, both runs AK and AS show an early phase with large local exponents, corresponding to the quasi-linear phase of large-scale instability (see also Grappin *et al.* 1988).

Using the local values of Lyapunov exponents evaluated in the time intervals $[t^0, t]$, we can calculate the corresponding Lyapunov dimension $d_\mathrm{L}(t)$, as defined in (8). Figure 5(*a–c*) shows for the three runs the convergence of the dimension $d_\mathrm{L}(t)$ with time, using different values of the time t^0 (the correspondence between labels and the value of t^0 is given on top of the figure). One sees that in all runs, there is an early phase during which the dimension is over-evaluated, compared to the further evolution. The case of run AP is the simplest: the figure shows that $d_\mathrm{L}(t)$ no longer depends on t^0, once t^0 is larger than 32: the asymptotic value of d_L should be close to 5. Convergence is not as fast for run AS (figure 5*c*), in which the dimension at time $t = 300$ systematically decreases with t^0, even at large values. Run AK (figure 5*a*) has the slowest convergence rate: at time $t = 300$, d_L is about 15 for t^0 between 20 and 100, it drops to $d_\mathrm{L} \approx 10$ when taking $t^0 = 160$, which comes from the fact that a very slow growth rate occurs for all ϵ_i in the period $t > 160$ (see figure 4*a*).

The succession of rapid and slow phases, i.e. of large and small local exponents, at times much larger than that of the quasi-linear phase, makes run AK interesting to study in more detail. We have counted six phases, and denoted them by roman numerals (included in the early linear phase) on figures 4(*a*), and also reported them on figures 3(*a*) and 5(*a*). The duration of these phases greatly exceeds the characteristic dynamical time, since the turnover time τ_NL is here about unity ($\tau_\mathrm{NL} \approx (k_\mathrm{i} U)^{-1} \approx 0.7$, with $k_\mathrm{i} \approx 1.5$ and $U \approx \sqrt{2E} \approx 0.9$). When comparing figures 4(*a*) and 3(*a*), we find that the 'fast' periods with large local exponents correspond to periods of bursts of activity in wavenumber shells $k > 1$ (figure 3*a*),

while periods with small exponents correspond to phases during which the spectrum is completely dominated by the first shell $k = 1$.

Such a feature has been found previously in two-dimensional flows for the (largest) error $\epsilon_1(t)$ corresponding to the first Lyapunov exponent λ_1 (Grappin *et al.* 1988; see also Ohkitani & Yamada 1989). A consequence of these variations is of course that the numerical evaluation of the Lyapunov exponents (and thus of the dimension) may depend strongly on the choice of the time interval $[t^0, t]$, so long as t is not much larger than the characteristic duration of these phases.

The preceding remarks suggest that the fluid oscillates between two distinct turbulent states and that their effective dimension may be evaluated separately, although the use of local exponents in the Kaplan–Yorke formula is probably questionable from a theoretical viewpoint. We have chosen the different starting times t^0 in figure 5(*a*) to coincide with the transition times between recurrent phases. One sees that the 'slow' phases (II, IV and VI) have a common local dimension of about 12, while the 'fast' phases (III and V) have a common local dimension of about 20. So, the fact that the dimension converges to about 17 (or 15 if one eliminates the early phase I) hides the fact that the attractor is probably made of two distinct subdomains of phase space.

Finally, we note that starting with a Kolmogorov flow leads very gradually to an initial fast phase corresponding to the early quasi-linear unstable phase; although the value of the dimension obtained by subtracting this initial phase (i.e. taking $t^0 \approx 20$) is probably nearer the true one, we shall not usually repeat this procedure in the following (i.e. we shall take $t^0 = 0$), since we are more interested in understanding the physics of the problem, than in obtaining precise values of the dimension.

4. Which are the pertinent degrees of freedom?

4.1. *The role of large scales in two-dimensional flows*

The preceding results show that, although there is no simple dependence of the Lyapunov dimension on Reynolds number, bursts of excitation at large scales raise the value of the exponents, and thus also lead to an increase of the instantaneous dimension of the attractor. This indicates that the number of active large scales might be an important factor in determining the value of the (asymptotic) Lyapunov dimension in these flows. Indeed, previous measurements of d_L in similar flows, indicated that the injection scale k_f^{-1} is a determining factor: decreasing this scale by a factor two (from $k_f = 2$ to $k_1 = 4$) at comparable Reynolds numbers led to a more than two-fold increase of the dimension d_L (GL87).

In order to elucidate this point, we consider forcing at a scale much smaller than previously, in a band of wavenumbers between 8 and 10: the forcing amplitudes are chosen randomly in this band, at the beginning of the run. We adopt this isotropic forcing in order to be able to compare directly our results with those of Lafon (1985), mentioned in §1. We checked that both kinds of forcing, either isotropic or harmonic, lead in fact to similar results.

As shown in table 2 (run AG), the corresponding dimension is very large: $d_L \approx 120$, at time $t = 80$. At that time, the large scales have all been excited (figure 1*d*), and a statistically steady state has been established (figure 2*d* and 3*d*). Note that the nonlinear turnover time is shorter than in previous runs: $\tau_{NL} \approx 0.4$, with $k_\lambda \approx 8$ and $U = \sqrt{2E} \approx 0.3$, so that $t = 80$ is about 200 turnover times. Note also that, although modes with $k \leqslant 8$ initially had zero excitation, energy has been transferred very

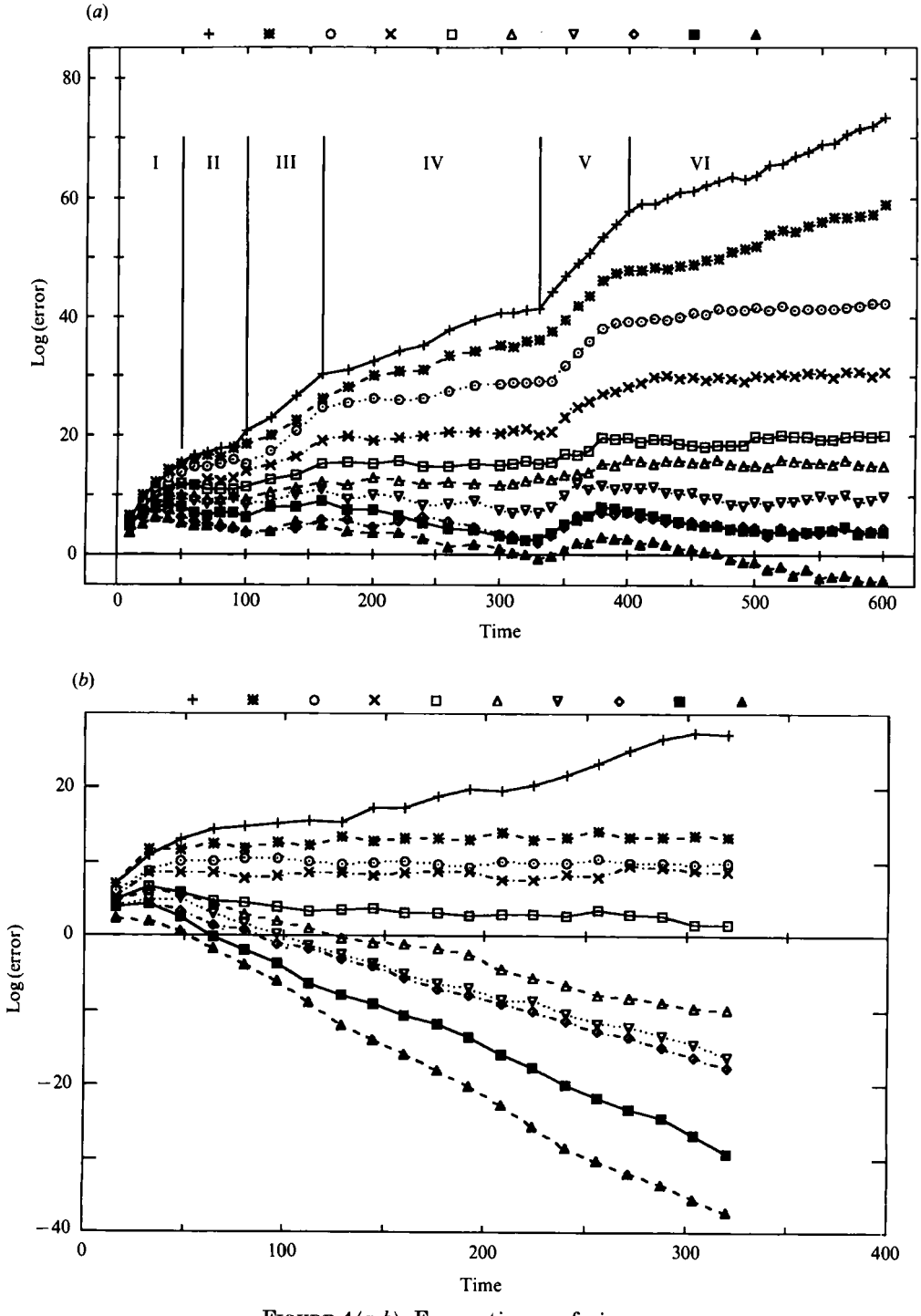

FIGURE 4 (a, b). For caption see facing page.

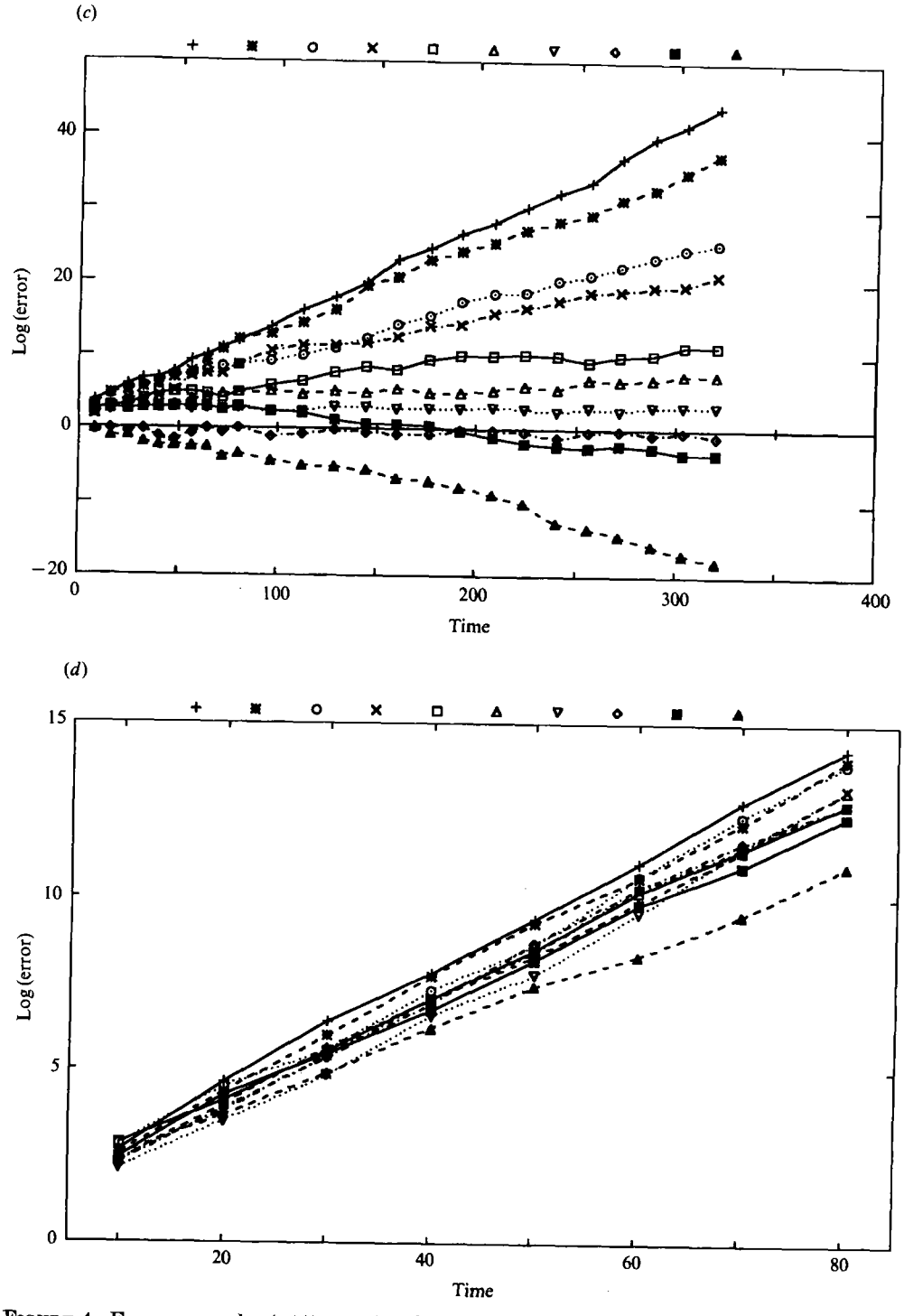

FIGURE 4. Error curves $\log(\epsilon_i(t))$ associated with the ten first Lyapunov exponents ($i = 1$ to 10). Symbols across the top of the figure indicate the order of the Lyapunov exponent, increasing from left to right. (*a*) Run AK, (*b*) run AP, (*c*) run AS, (*d*) run AG.

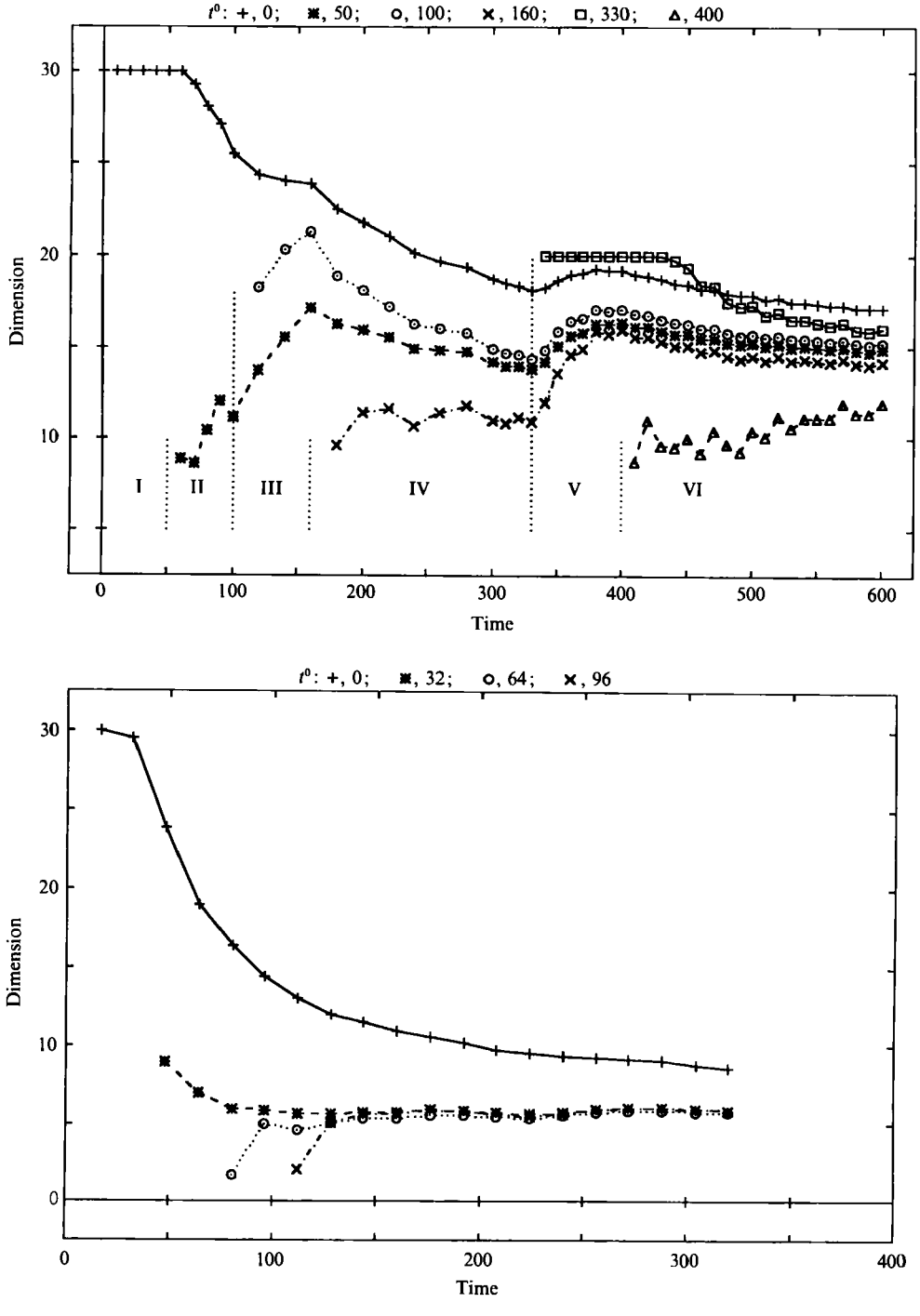

FIGURE 5(*a*,*b*). For caption see facing page.

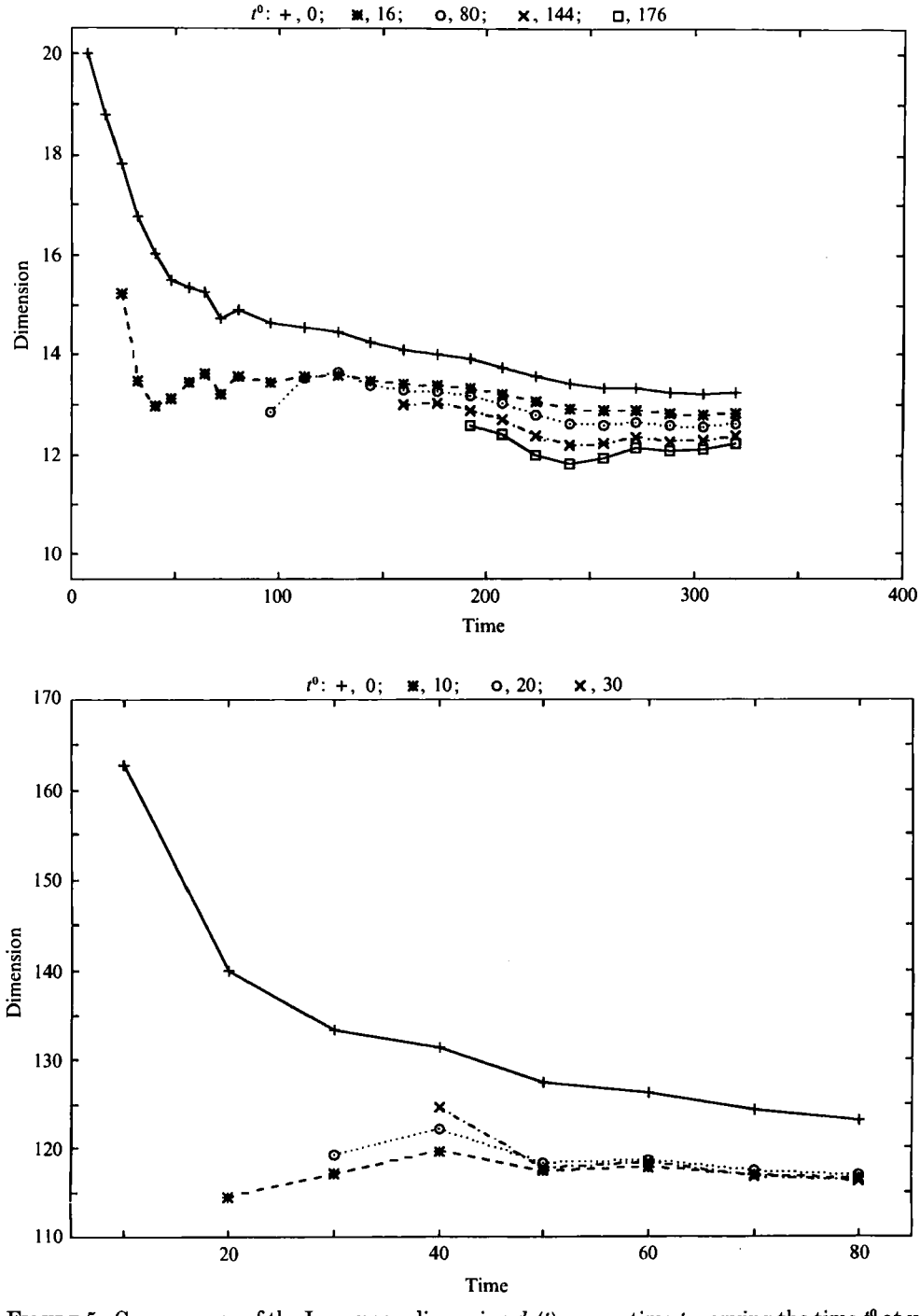

FIGURE 5. Convergence of the Lyapunov dimension $d_L(t)$ versus time t, varying the time t^0 at which the evaluation starts. The upper legend indicates the value of t^0. (*a*) Run AK, (*b*) run AP, (*c*) run AS, (*d*) run AG.

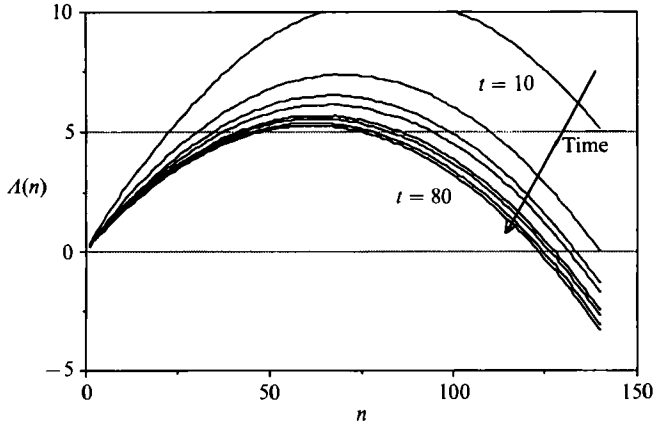

FIGURE 6. Spectrum of cumulated Lyapunov exponents $\Lambda(n)$, versus n, at times: $t = 10$ to 80 (run AG).

quickly (in fact in a time shorter than one) on the largest scales (see Grappin *et al.* 1988). The average integral Reynolds number is about 10, with the viscosity being about the smallest compatible with a fair truncation (see figure 1*d*). The velocity field is completely isotropic at small scales, and almost isotropic at large scales.

The convergence of $d_L(t)$ is seen to be satisfactory at that time, when one starts with $t^0 = 10$ (cf. figures 4*d* and 5*d*). The whole spectrum of (cumulated) exponents $\Lambda(n)$ measured for this run is shown in figure 6, for different times, from $t = 10$ to $t = 80$ (with $t^0 = 0$).

A comparison with Lafon's (1985) results is in order. Lafon used a counting method to measure the correlation dimension d_c of the same flow (same resolution, same forcing at the same scale). He varied the viscosity ν, starting from the critical value for the instability to set in, down to the smallest compatible with the resolution (64^2), and obtained a monotonic rise to the correlation dimension d_c with $1/\nu$, with a maximum $d_c = 25$ (at the smallest viscosity). This value is almost five times smaller than the Lyapunov dimension we found for the same flow at the same resolution. Note that Lafon mentions in his thesis only the viscosity, but no global measure of the velocity which would allow the evaluation of a (dimensionless) Reynolds number. Nevertheless, we think that the values given by Lafon are smaller than our estimation of dimension because of his choice of algorithm. Indeed, Atten *et al.* (1984) showed that a counting algorithm cannot obtain more than lower bounds of the attractor dimensions, once the dimension is much larger than, say, 5 ('border effect'). Comparable discrepancies (i.e. $d_c \ll d_L$) between Lyapunov and correlation dimension in the case of a model of developed turbulence have been reported in Grappin *et al.* (1986).

The variation of the dimension with injection wavenumber is shown in figure 7, which gathers together the results of the four runs AK, AP, AS and AG, and the previous results with $k_f = 2$ reported in GL87. It shows that the maximum Lyapunov dimension that can be reached (while still keeping the small scales well resolved) scales approximately as k_f^2. More precisely, it is bounded above by the number of degrees of freedom contained in scales larger than k_f^{-1}, which is $N_{LS} \approx \pi k_f^2$ (denoted by a straight line in figure 7).

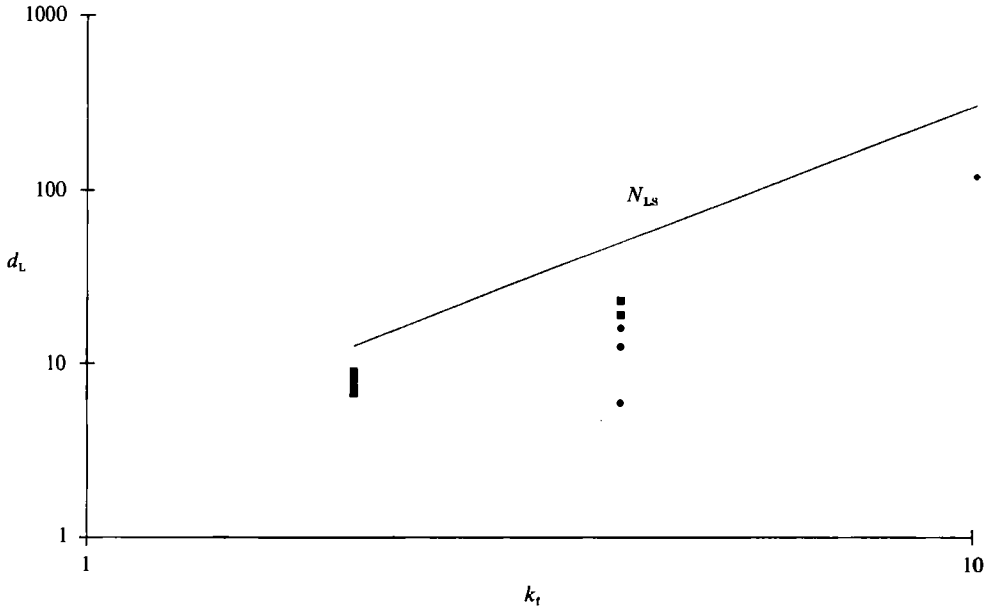

FIGURE 7. Dimension d_L versus injection wavenumber k_f in two-dimensional flows. Results for runs of type A (black diamonds) and results reported in GL87 (squared symbols) are shown together. The straight line is the number N_{LS} of degrees of freedom with wavenumber smaller or equal to the forcing wavenumber k_f, namely about πk_f^2. The three abscissae are $k_f = 2, 4$ and $k_f = 8$–10 (run AG).

Run	Bbx	Bzz	Bcg	Bcc	Bzs	Bbg	Bbb	Bze
Res	64^2	64^2	128^2	128^2	64^2	64^2	64^2	64^2
p	2	2	2	2	4	4	4	8
ν_p	3.05×10^{-4}	6.10×10^{-5}	3.81×10^{-5}	7.63×10^{-6}	2.9×10^{-10}	1.5×10^{10}	7.6×10^{-11}	2.65×10^{-22}
ν	[0.3]	[0.06]	[0.16]	[0.03]	[0.3]	[0.16]	[0.08]	[0.3]
N_{dis}	17	6	34	13	8	6	4	4
dt	0.08	0.08	0.04	0.04	0.08	0.08	0.08	0.08
τ_{NL}	0.51	0.46	0.45	0.44	0.44	0.44	0.43	0.43
k_λ	2.39	2.33	2.32	2.3	2.31	2.29	2.28	2.26
k_p	2.57	2.66	2.68	2.79	5.09	5.31	5.52	12.5
R_p	160	814	1287	5.9×10^3	3.8×10^4	5.7×10^4	8.5×10^4	1.3×10^5
k^*	3	7	7	9	13	13	13	20
N^*	28	154	154	255	531	531	531	1257
d_L	0	5.4	5.5	12	21	27	30	50

TABLE 3. Two-dimensional runs with modified dissipation. p is the power of the Laplacian (see (1c); ν is the 'equivalent' viscosity and ν_p the hyper-viscosity (see text). N_{dis} is the wavenumber width of the dissipative range, dt is time step. Injection wavenumber is $k_f = 2$; the forcing amplitude is $f = 0.1$. The middle section gives some time-averaged quantities, at time $T = 80$: nonlinear turnover time τ_{NL}, Taylor and modified wavenumber k_λ and k_p, modified Reynolds number R_p. k^* is the (visually estimated) largest wavenumber of the quasi-inertial range (see text and figure 9), and $N^* = \pi k^{*2}$. The last line gives the Lyapunov dimension at time $t = 120$.

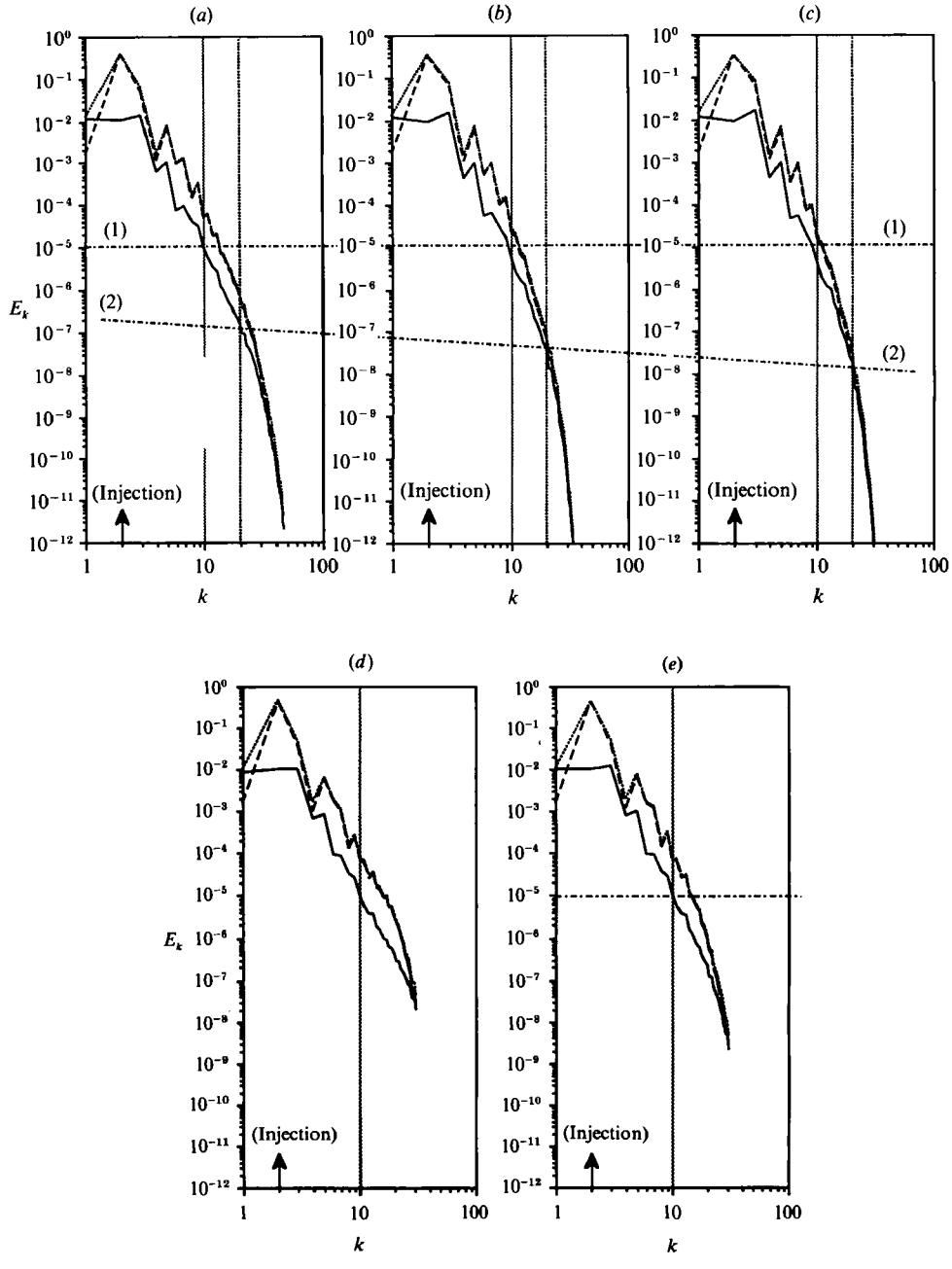

FIGURE 8(*a–e*). For caption see facing page.

4.2. *Attractor's dimension and size of the inertial range (two-dimensional flows with artificial dissipation)*

The scaling of maximum dimension d_L with the number of large-scale modes illustrates the importance of large scales in two-dimensional flows. However, we know that small scales are important too, be it only because we have to take them into account in the numerical simulations. We consider in this subsection the

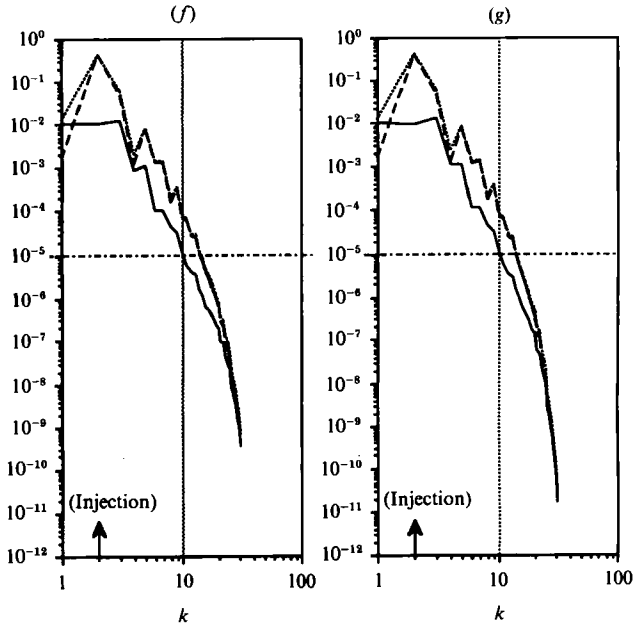

FIGURE 8. Time-averaged energy spectra E_k in two-dimensional flows with artificial dissipation (at time $t = 80$). Continuous lines indicate the x-component, dashed lines the y-component, and dotted lines the total component. Line (1) joins the spectra at wavenumber $k = 10$, line (2) joins the spectra at $k = 20$. (*a*) Run Bcc, (*b*) run Bcg, (*c*) run Bzz, (*d*) run Bze, (*e*) run Bbb, (*f*) run Bbg, (*g*) run Bzs.

artificial dissipation terms (1*c*), which should enhance the relative importance of small scales, compared to the previous runs. First, the friction term should reduce the relative importance of the largest scales; second, since the dissipation is peaked very strongly on the smallest scales, it gives the flow an opportunity to develop an inertial range.

The flow is driven at the largest possible forcing scale, $k_f = 2$ (the case $k_f = 1$ is linearly stable) and the forcing amplitude is $f = 0.1$. From (3), the amplitude of the equilibrium Kolmogorov flow is thus 0.8 (the r.m.s. value is thus 0.56). The initial conditions are the same for all runs (a white noise). The only parameters to be varied are the small-scale dissipation parameters, p and the hyperviscosity ν_p (see table 3).

These flows show several specific properties. Some are due to the friction term $\nabla^{-2}\psi$, which leads to a maximum damping at the largest scale. There is a minimum at $k = 1$ in all spectra (figure 8). Next, the stationary (turbulent) value of the r.m.s. velocity is larger (about unity) than its (linear) equilibrium value of 0.56 given above because a well-developed spectrum induces a lower dissipation rate than the equilibrium flow (3). Note also that the y-energy dominates the spectrum even at relatively small scales (compare figures 8 and 1).

The most interesting property is that, with $p > 1$, the hyperviscosity concentrates small-scale dissipation in a narrow band of wavenumbers. The width $N_{\rm dis}$ of this band has to be kept to a minimum, by taking ν_p large enough (see table 3; $N_{\rm dis}$ is the number of wavenumbers for which the dissipation time $(\nu_p k^{2p})^{-1}$ is shorter than the nonlinear time $(kU)^{-1} \approx k^{-1}$, so that the number of 'dissipative' modes is about $2\pi(k_{\rm max} - 1)N_{\rm dis}$).

For $k \leqslant 5$, the total energy spectra are comparable for all runs; the same is true for

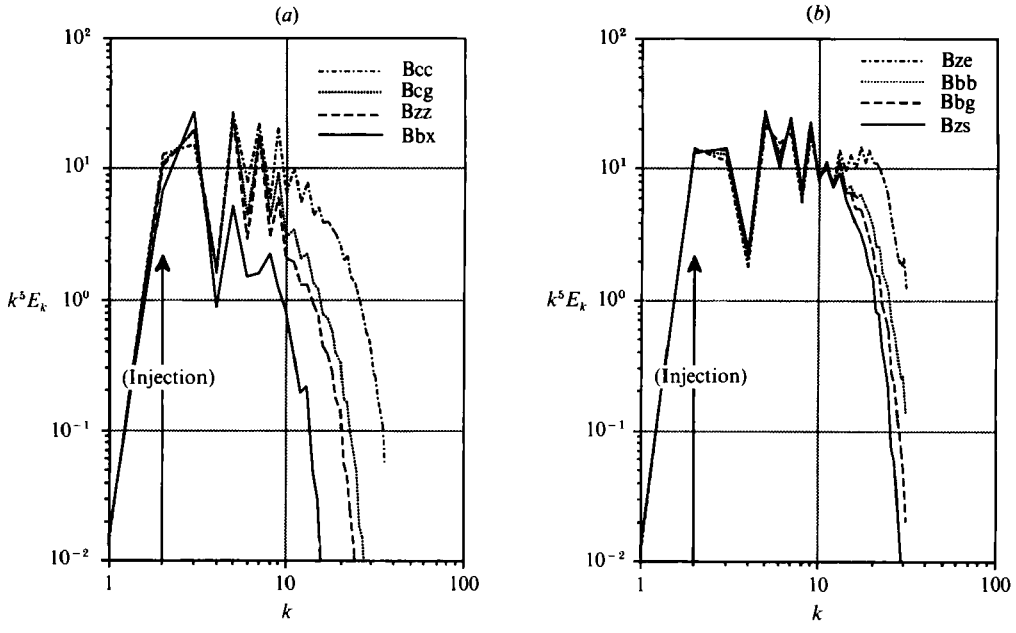

FIGURE 9. Superposed time-averaged total energy spectra (multiplied by k^5) in two-dimensional flows with artificial dissipation (type B), at time $t = 80$. (*a*) Laplacian squared ($p = 2$), (*b*) $p = 4$ and 8.

the x-component of the spectrum at least for $k \leqslant 10$ (see the straight horizontal line (1) in figure 8). However, the y-component of the spectrum is more sensitive to the variations of the hyperviscosity. More generally, rising p or decreasing ν_p extends the width of the non-dissipative range, which is more or less common to all runs. A part at least of this non-dissipative range can be fitted reasonably well by a power law, with slope around -5. We have plotted in figure 9 the superposed compensated spectra k^5E_k (separately runs with $p = 2$ on the one hand, and $p = 4$ and 8 on the other). It appears that all compensated spectra show a common flat range, extending from $k = k^0$ towards a maximum wavenumber k^* which depends on the diffusivity. The oscillations, and particularly the large gap at $k = 4$, are probably due to the peculiar energy balance of the flow which experiences both injection and damping at large scales. Accordingly, no particular importance should be given to the particular -5 slope: the only point which matters here is that an approximate power-law range with variable size appears. When $p = 2$, the width k^* of the k^{-5} range appears to increase as ν_p decreases (figure 9*a*). We tentatively evaluate k^* by mere visual inspection; we find $k^* = 3, 7, 7, 9$, with ν_p decreasing from 3×10^{-4} to 8×10^{-6}. When $p = 4$, we find $k^* = 13$ for the three values of ν_4 considered, and $k^* = 19$ when $p = 8$ (figure 9*b*).

Note that the independence of the energy level at large scales from the small-scale dissipation parameters probably owes much to the friction term which, at wavenumber $k_f = 2$, fixes locally the energy injection and thus the enstrophy transfer rate to smaller scales (compare the large scales in figures 8 and 1).

The convergence of the Lyapunov dimension in the different runs versus time is shown in figure 10. No effort has been made to subtract the initial transients. Note that, in spite of the friction term which might result in a lower dimension, d_L becomes equal to the number of large-scale degrees of freedom ($N_{LS} = 12$) with the smallest

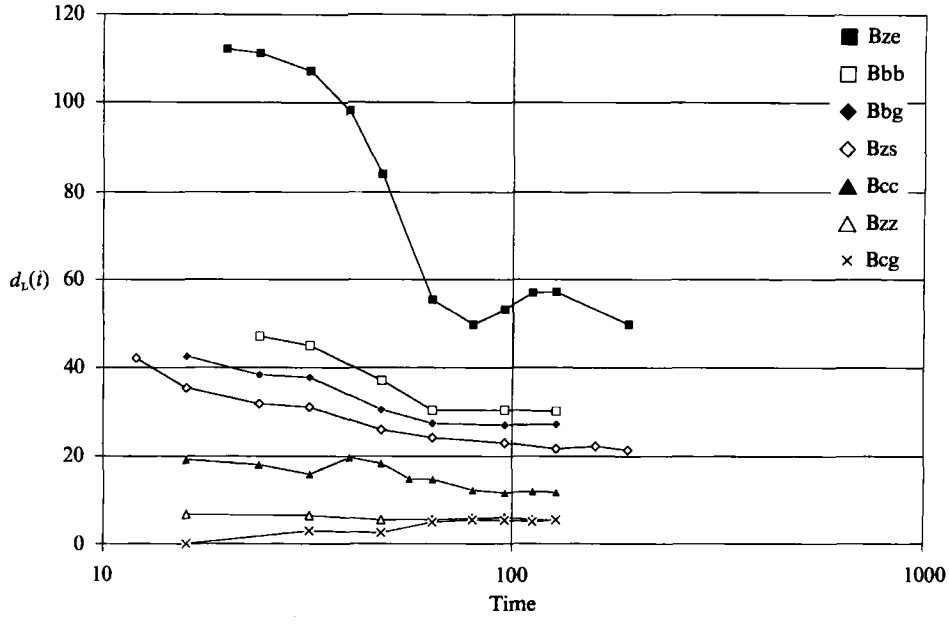

FIGURE 10. Convergence of Lyapunov dimension $d_L(t)$ with time in two-dimensional flows with artificial dissipation (type B). Abcissae is time in logarithmic units.

value of ν_p when $p = 2$ (run Bcc), and is always above N_{LS} with $p = 4$ and 8. For comparison, note that the maximum dimension obtained with $k_f = 2$ in flows with standard dissipation (and maximum Reynolds number compatible with the resolution) is 9 (GL87).

It is interesting to see how d_L rises when the flow becomes more turbulent. To evaluate the intensity of turbulence, a possibility is to use the modified Reynolds number R_p: we see that the dimension d_L rises monotonically with R_p, although not very regularly (table 3). However, the definition (4) of R_p is somewhat arbitrary, and has no physical basis. So we prefer to compare d_L directly with the width k^* of the inertial range, though its evaluation is clearly approximate.

One sees that both d_L and k^* grow together, and that for chaotic flows ($d_L > 0$), the relation is approximately linear (see figure 11). For comparison, table 3 shows that the number of degrees of freedom contained within k^* is $N^* = \pi k^{*2}$, which is always more than an order of magnitude above d_L.

4.3. *Three-dimensional flows*

We report in this subsection the results of three simulations of three-dimensional flows with standard dissipation. The resolution is 16^3. Note that measuring, say, 128 exponents in such flows requires the same amount of memory as solving a two-dimensional flow with resolution 512×1024, but the CPU time per nonlinear time is much smaller in a 16^3 flow, being built on much larger scales ($k_{max} = 8$) than in a 512×1024 flow.

The results are reported in table 4. The three runs differ in the type of forcing and the viscosity. Forcing is a perturbation of the Kolmogorov harmonic forcing (1*e*) in run CY ($k_f = 2$, $U_x \approx \cos(2y)$); it is isotropic in runs CE and CJ in the wavenumber band from $1 \leqslant k_f \leqslant 2$. The difference in forcing shows in the time-averaged spectra shown in figure 12: isotropic forcing leads to isotropic flows. Note that the viscosity

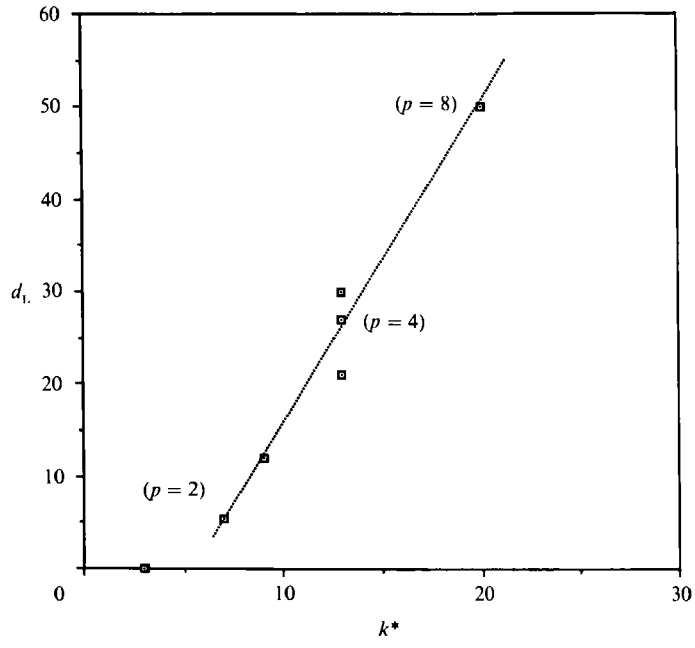

FIGURE 11. Lyapunov dimension d_L versus width of the inertial range k^* in two-dimensional flows with artificial dissipation (type B).

Run	CY	CE	CJ
Res	16^3	16^3	16^3
ν	0.01	0.01	0.005
Forcing	harmonic	isotropic	isotropic
dt	0.02	0.02	0.02
T	240	160	80
U	0.29	0.29	0.3
R_i	18	15.5	27
R_λ	12	11	17.5
k_λ	2.5	2.6	3.5
N	2836	2836	2836
N_{LS}	67	67	67
d_L	48	57.5	105

TABLE 4. Three-dimensional runs (with standard dissipation). ν is viscosity, dt is time step, T is the integration time. U, R_i, R_λ and k_λ are time-averaged quantities. N is the total number of degrees of freedom after isotropic truncation in Fourier space, $N_{LS} = \frac{8}{3}\pi k_f^3$ is the number of degrees of freedom with wavenumber smaller than the forcing one (which is $k_f = 2$), d_L is the Lyapunov dimension at time T.

in run CJ is half that of runs CY and CE. This value is somewhat too low for the resolution; indeed, the comparison of the three spectra in figure 12 indicates that the small scales are well resolved in runs CY and CE, but might not be so well resolved in run CJ, which perhaps shows levels of excitation on the largest wavenumber which are too high.

Figure 13 gives some details on run CE. Figure 13(a) shows the evolution of the main relevant quantities for run CE (cf. figure 2; note however that the dotted lines now denote the z-component of the various quantities, and not the total component

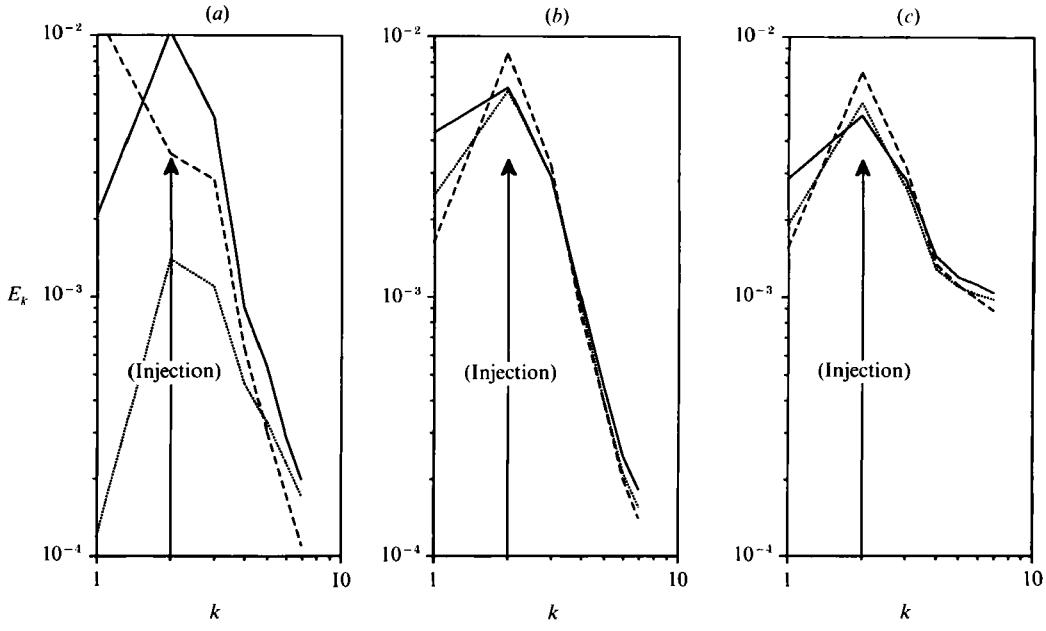

FIGURE 12. Time-averaged energy spectra E_k of three-dimensional flows. Continuous lines indicate the x-component, dashed lines the y-component, and dotted lines the z-component. (a) Run CY at $t = 240$, (b) run CE at $t = 160$, (c) run CJ at $t = 80$; see table 4.

as in figure 2). One sees from the k_λ and k_d curves that the small scales of the flow show a brief period of larger excitation (around time $t = 10$) after which a quasi-stationary state is established. The first 20 error curves are shown in figure 13(b): one sees that, even at time 160, the ordering of the exponents is far from perfect; note however that the global ordering is correct, as is shown by the gentle aspect of the cumulated exponent $\Lambda(n)$ curve (figure 13c) from times 40 to 160. Note that there is no indication of a complicated attractor's structure as in run AK (figure 13b). The dimension is seen to converge around 50 (figure 13d).

The dimension d_L is respectively 48, 57 and 105 in runs CY, CE and CJ. Thus, notwithstanding the difference in anisotropy of the flows, runs CY and CE lead to comparable values of d_L. On the other hand, the low viscosity has the immediate effect of increasing d_L by a factor two in run CJ. Note that run CJ has been integrated up to a shorter time than the two other runs, but that the dimension converges reasonably at around 100, as shown in figure 14.

The values of d_L which we obtain for the two flows CY and CE that are best resolved are thus again bounded by the number of large-scale modes which is here $N_\mathrm{LS} \approx \frac{8}{3}\pi k_\mathrm{f}^3 \approx 67$ (with $k_\mathrm{f} = 2$). The total dimension of the phase space is $N = 2836$.

Some comments on the related results of Keefe, Moin & Kim (1989) are in order. These authors find a very high Lyapunov dimension in a simulation of a three-dimensional turbulent Poiseuille flow: d_L between 360 and 400 for a resolution of $16 \times 32 \times 8$ points, at a Reynolds number of 3200. They conclude that 'because the resolution ... was coarse in homogeneous directions of the flow, and the spatial domain small', this dimension is 'a lower bound on its true value at this Reynolds number'. They thus suggest that adding more modes to the numerical simulation would give a system with a still larger dimension. However, this is not necessarily true. Indeed, it seems to us difficult to simulate flows at such high Reynolds numbers

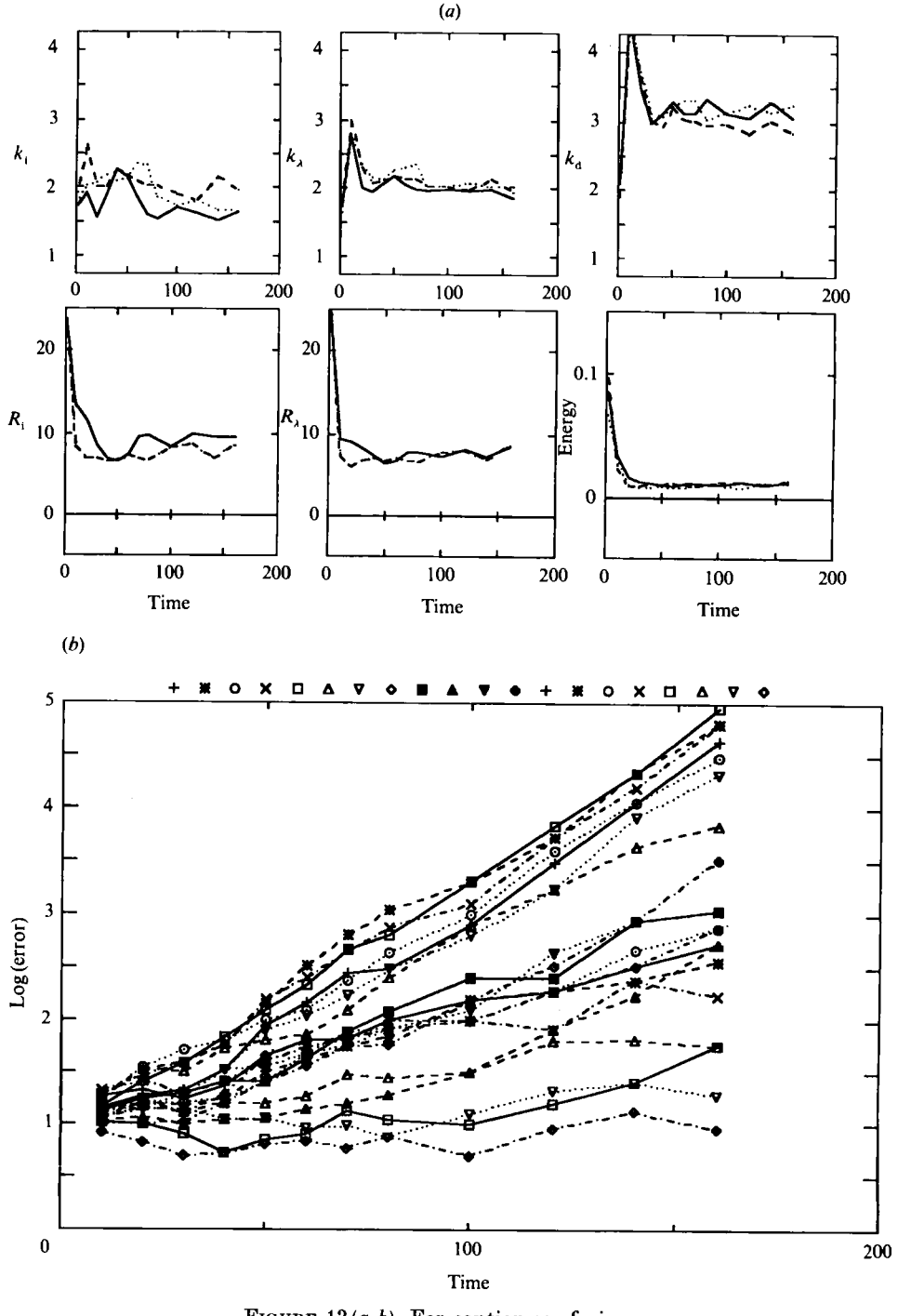

FIGURE 13(a,b). For caption see facing page.

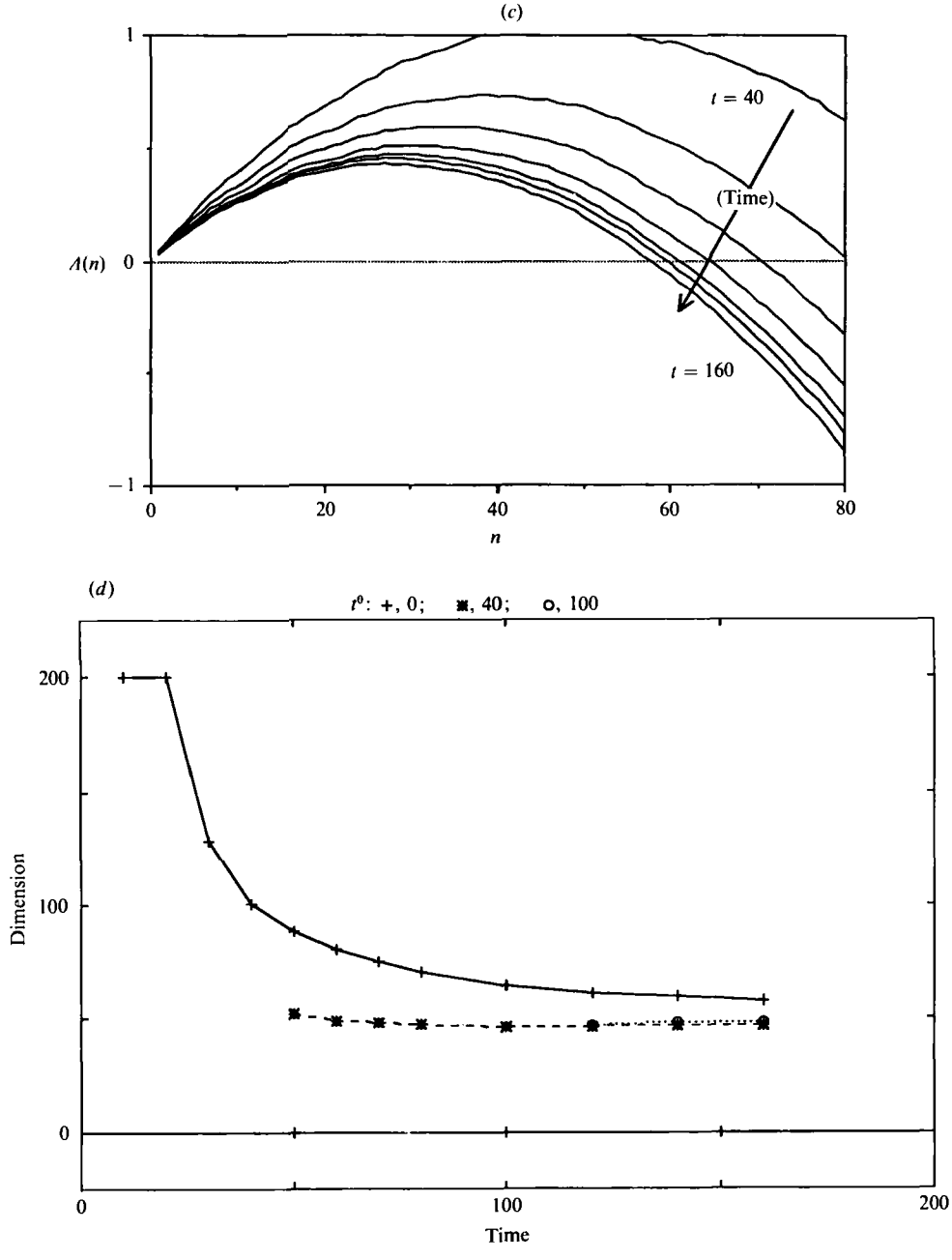

FIGURE 13. A three-dimensional flow (run CE). (*a*) Global parameters versus time (continuous, dashed and dotted lines respectively denote x-, y- and z-components). (*b*) Error curves $\log(\epsilon_i(t))$ associated with the first 20 Lyapunov exponents ($i = 1$ to 20). Symbols across the top indicate the order of the Lyapunov exponent, increasing from left to right. (*c*) Spectrum of cumulated Lyapunov exponents $\Lambda(n)$, versus n, at times: $t = 40, 60, 80, 100, 120, 140, 160$. (*d*) Lyapunov dimension $d_L(t)$ versus time, varying the starting time t^0.

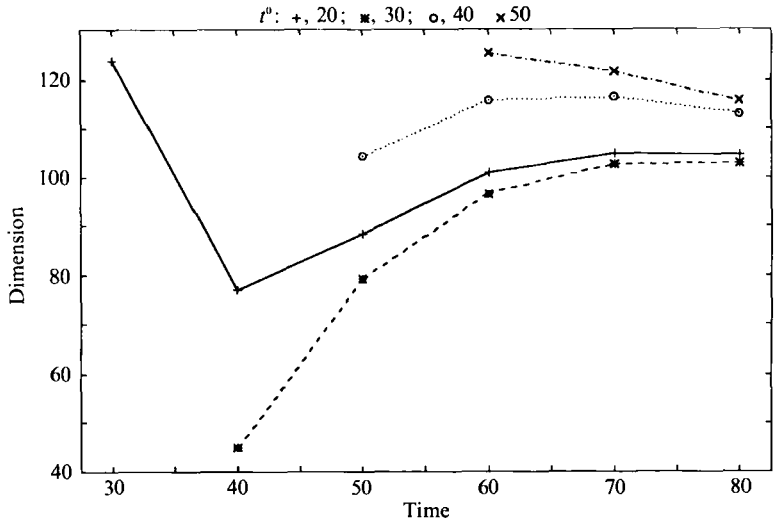

FIGURE 14. Converge of Lyapunov dimension $d_L(t)$ with time (three-dimensional flow, run CJ).

with such a low resolution, and still to have well resolved small scales. (The authors do not give any information that would allow the reader to assess this point.) If, as we think, the flow is not well resolved, then adding more modes (without changing the dissipation parameter) will then allow the artificial small-scale excitation to decrease, which would give a result opposite to that conjectured by the authors, i.e. would reduce the dimension instead of increasing it. Let us recall that it is always possible to obtain a dimension equal to the maximum dimension of the phase space, $d_L = N$: it is sufficient to take $\nu = 0$ (or, in practice, ν much lower than the minimum value adapted to the resolution); but then, the numerical system does not describe a turbulent flow, but the so-called 'absolute equilibrium' state, which is qualitatively different (see also Grappin *et al.* 1986; and GL87).

4.4. *A study of the basis of Lyapunov vectors*

If we admit that the fluid state converges towards an attractor of finite (small) dimension d_L, can we find truncated expansions of the flow on a special basis, such that a truncation of order d_L is enough to represent the flow? We investigate in this subsection whether the basis of Lyapunov vectors, i.e. the orthonormal set of linear solutions from which Lyapunov exponents are deduced, provides such a compact basis, following a suggestion by Kraichnan (1987).

What kind of relation between the nonlinear field and its set of Lyapunov vectors can we expect? Recall the two-dimensional case of a passive scalar ζ, which obeys an equation identical to the linearized Navier–Stokes equation (4) for $\delta\psi$, except for the third term of the left-hand side which is missing. The spatial configuration of ζ is known to be very near to that of the nonlinear field ψ, although the spectra of both quantities may be completely different, because the coherent structures which are present in the nonlinear field ψ are absent in the passive-scalar field ζ (see Babiano *et al.* 1987). Thus linear solutions (as are the Lyapunov vectors) might be close enough to the nonlinear solution ψ to provide a good basis.

We consider here the case of two-dimensional flows only. Let us examine first the simplest case of the conservative system (with no forcing and zero viscosity). This is not a realistic model for fluid turbulence since there is no dissipation to reduce the

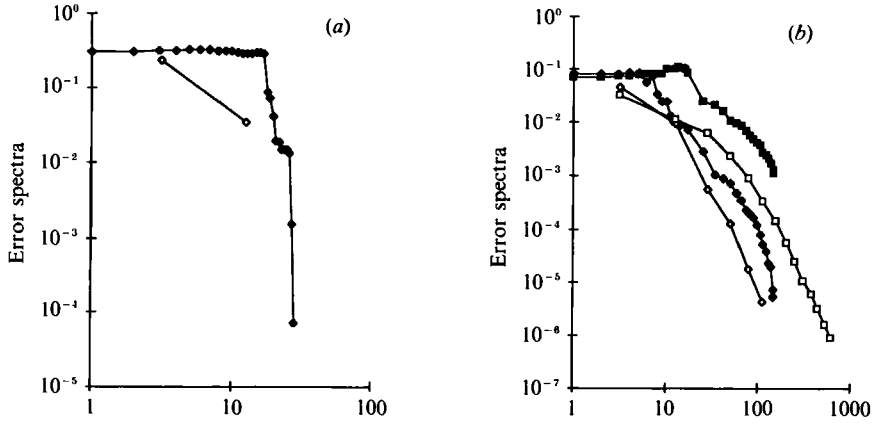

FIGURE 15. Comparison of truncated expansions of an instantaneous two-dimensional flow: plots of the truncation error spectra on the Lyapunov vectors basis (black symbols) and on the Fourier basis (white symbols). The abcissae is of the order of the truncation. For the Lyapunov basis it is the number of Lyapunov vectors, for the Fourier basis the number of degrees of freedom with wavenumber smaller than or equal to k (i.e. about πk^2), k taking integer values from 2 to $k_{\max}-1$ ($k_{\max}=\frac{1}{2}n$, if n is the linear resolution). (*a*) Inviscid case, resolution 8^2 (run AL): Lyapunov dimension is equal to the total number of degrees of freedom of the system $N=28$. (*b*) Viscous case, resolution 16^2 and 32^2: runs AN (diamonds) and AP1 (squares) respectively.

small-scale excitation, but it is an interesting system in itself (run AL in table 2). As has been mentioned in §4.3, in the inviscid case the Lyapunov dimension must be equal to the total dimension of the system in phase space. We consider here a resolution of 8^2. The corresponding dimension of phase space is then $N=28$, corresponding to 14 complex modes (note that the maximum wavenumber is $k_{\max}=3$), which is enough for the system to be chaotic.

We plot on figure 15(*a*) the spectrum of (squared) truncation errors made by approximating the field at time $T=200$ by the first n Lyapunov vectors. The truncation error spectrum should vanish when n approaches $N=28$. The fact that it is not exactly zero is related to the orthonormalization procedure. The truncation error is seen to be large (comparable with the total energy, which is 0.3) and almost constant, while n is smaller than $\frac{1}{2}N=14$; it drops abruptly afterwards. Thus, the first-half of the Lyapunov vectors, which are, roughly speaking, the unstable ones, all contain a substantial part of the energy of the field. The second half (the stable directions) contain almost no energy. We plotted the curve of truncation errors of the standard Fourier representation in the same figure for comparison. The two abscissae are the number of Fourier modes in the disks $k\leqslant 1$ and $k\leqslant 2$ (in the disk $k\leqslant k_{\max}=3$ the truncation error is zero since there is no truncation). It is seen that the Fourier representation converges much more quickly than the Lyapunov one.

We next consider two runs with finite viscosity (runs AN and AP1, in table 2), at resolutions 16^2 and 32^2. In both cases, we calculate 148 exponents, which represent all the degrees of freedom in the first case, and a substantial fraction (148 over $N=708$) in the second case. Results are presented on figure 15(*b*). We plot as previously the spectrum of squared truncation errors (black symbols) and the same spectrum for Fourier representation (white symbols). We observe now an error of about 100% for the Lyapunov representation when the order n of the truncation is lower than the computed dimension d_{L} (instead of half the dimension as in the previous inviscid

case), which is respectively $d_L \approx 8$ and 29 for runs AN and AP1. However, in contrast with the inviscid case (run DL) previously considered, the decay of the truncation error is not abrupt at larger values of n. Instead, the spectrum approaches a powerlaw, similar both for the Lyapunov and Fourier representation, but again larger at all wavenumbers for the Lyapunov representation.

5. Summary and conclusion

We have studied the turbulent state developed by an incompressible flow submitted to a constant periodic force, trying to characterize this turbulent state by the spectrum of Lyapunov exponents of the flow (and the associated errors), and by the Lyapunov dimension of the attractor.

(i) Our first result concerns the interpretation of the time evolution of the instantaneous exponents and dimension. It is of course well known that large initial transients often occur during the calculation of Lyapunov exponents in dynamical systems; these transients correspond to persistent fluctuations in the instantaneous exponents. In general no particular attention is given to them. Grappin *et al.* (1988) have however shown that in two-dimensional Navier–Stokes flows, the permanent fluctuations in the first instantaneous Lyapunov exponent (the 'error', or largest stretching rate) do have a physical significance: they are associated with abrupt changes in the characteristic eddy turnover time, which represents the internal clock of the fluid. We generalize this result here by showing that the whole spectrum of instantaneous positive exponents rises when the characteristic turnover time rises, which manifests itself by changes in the energy spectrum at large scale. In a particular case (run AK) we find that the flow explores successively two distinct subdomains in the attractor, the recurrence time being much larger than the dynamical timescale of the flow. If we tentatively use the Kaplan–Yorke formula in each separate subdomain, we find that the 'large' one has a dimension $d_L \approx 20$, and shows approximate energy equipartition between all scales larger than the injection scale ($1 \leqslant k \leqslant k_f = 4$, see figure 3*a*), while in the 'small' subdomain, we find $d_L \approx 12$, and the energy is essentially concentrated on the largest scale $k = 1$.

(ii) The correlation between the large-scale spectral features and instantaneous exponents is a clear indication that in two-dimensional flows the 'pertinent' scales which may contribute to the attractor's dimension are above the injection scale. This is indeed confirmed by our second result which is that, when one varies the injection scale, the Lyapunov dimension of these flows is bounded above by the number N_{LS} of degrees of freedom contained above the injection scale (figure 7).

(iii) These results concern two-dimensional flows with maximum resolution 128^2, and maximum (average) Reynolds number about 80. When an inertial range is present, which is obtained here by artificial dissipation, the dimension of two-dimensional flows may be much higher than N_{LS}. d_L rises with the size k^* of the inertial range; however, it only rises linearly (figure 11), so that the dimension is much smaller than the number of degrees of freedom contained in the inertial range. Note that the artificial dissipation comprises a friction term which damps the largest scales, and so partly determines the position of the curve in figure 11, but should not modify the linearity of the $d_L(k^*)$ relation.

(iv) In three-dimensional flows, the dimension is of the order of or a little larger than N_{LS}. However, d_L is only larger than N_{LS} in a flow in which the small scales are not well resolved (run CJ). Note that the very limited resolution does not allow a scaling with the number of large-scale modes to be sought, as can be done in two-

dimensional flows, and that, of course, no inertial range can be expected with resolution 16^3.

(v) Finally, we find that the convergence of truncated expansions of the instantaneous flow on the basis of Lyapunov vectors is worse than on the standard Fourier basis. A similar negative result has been recently reported by Keefe (1989) on the decomposition of the solution of the Ginzburg–Landau equation on the basis of its Lyapunov vectors; he also concludes that the Lyapunov basis is the best one to represent the time derivative of the nonlinear solution. These results are not unreasonable, but leave open the problem of finding a reduced representation of a turbulent flow with a small attractor's dimension.

The fact that standard flows are bounded by the number of large scales is perhaps not a surprise, since we know that there cannot be any substantial inertial range in these flows at the resolution studied here. However, the slow rise of d_L with the size k^* of the inertial range in flows with modified dissipation is more peculiar, and needs interpretation, since it contradicts theoretical predictions, either based on intuition (Landau & Lifshitz 1971) or much more sophisticated (Constantin *et al.* 1985). Note this is not due to a shortcoming of the computational method, since similar computations on models of turbulence have given 'large' dimensions (Manneville 1985; Grappin *et al.* 1986; Yamada & Ohkitani 1988).

Our general conclusion is that the small scales have, relatively to large scales, not much importance in determining the dimension of the turbulent flows we have studied, even when an inertial range is present. It is tempting to interpret this as a signature of the presence of coherent (but chaotic) structures at large scales, the role of small scales being purely passive. Legras *et al.* (1988) and Babiano *et al.* (1987) have indeed convincingly shown that the origin of the difficulty found in reproducing the self-similar spectra predicted by Kolmogorov-like theories in two-dimensional numerical simulations lies in the organized large-scale eddies which develop in two-dimensional flows. Such coherent structures are not taken into account by a self-similar theory. Now, the theories and models that predict large attractor dimensions use in one way or another a 'built-in' hypothesis of self-similarity, and thus do not take coherent structures into account: it is not surprising that they predict Lyapunov dimensions larger than those obtained via numerical computations.

One of us (R.G.) acknowledges a stimulating discussion with H. Chaté and P. Manneville at an early stage of this work. We thank A. Mangeney and M. Velli for very useful remarks and criticism when reading the revised version of the manuscript. We thank the scientific committee of the Centre de Calcul Vectoriel pour la Recherche (CCVR) who provided the computational facilities. We are grateful to the referees who helped to improve the clarity and content of the paper.

REFERENCES

Atten, P., Caputo, J. G., Malraison, B. & Gagne, Y. 1984 Détermination de dimension d'attracteurs pour différents écoulements. *J. Méc. Theor. Appl., Numéro Spécial*, p. 133.

Babiano, A., Basdevant, C., Legras, B. & Sadourny, R. 1987 Vorticity and passive-scalar dynamics in two-dimensional turbulence. *J. Fluid Mech.* **183**, 379.

Basdevant, C., Legras, B., Sadourny, R. & Beland, M. 1981 A study of barotropic model flows: intermittency waves and predictability. *J. Atmos. Sci.* **38**, 2305.

Benettin, G., Galgani, L., Giorgilli, A. & Strelcyn, J.-M. 1980 *Meccanica* **15**, 10.

Brachet, M. E., Meneguzzi, M., Politano, H. & Sulem, P. L. 1988 The dynamics of freely decaying two-dimensional turbulence. *J. Fluid Mech.* **194**, 333.

CONSTANTIN, P., FOIAS, C., MANLEY, O. P., TEMAM, R. 1985 Determining modes and fractal dimension of turbulent flows. *J. Fluid Mech.* **150**, 427.

GALLOWAY, D. & FRISCH, U. 1987 A note on the stability of space-periodic Beltrami flows. *J. Fluid Mech.* **180**, 557.

GRAPPIN, R. & LÉORAT, J. 1987 Computation of the dimension of two-dimensional turbulence. *Phys. Rev. Lett.* **59**, 1100 (referred to herein as GL87).

GRAPPIN, R. & LÉORAT, J. 1989 Lyapunov dimension of homogeneous shear flows. In *Conf. on Nonlinear Dynamics, Bologna* (ed. G. Turchetti). Singapore: World Scientific.

GRAPPIN, R., LÉORAT, J. & LONDRILLO, P. 1988 Onset and development of turbulence in two-dimensional periodic shear flows. *J. Fluid Mech.* **195**, 239.

GRAPPIN, R., LÉORAT, J. & POUQUET, A. 1986 Computation of the dimension of a model of fully developed turbulence. *J. Phys. Paris* **47**, 1127.

GREEN, J. S. A. 1974 Two-dimensional turbulence near the viscous limit. *J. Fluid Mech.* **62**, 273.

KAPLAN, J. L. & YORKE, J. A. 1979 In *Functional Differential Equations and Approximations of Fixed Points*, p. 228. Springer.

KEEFE, L. 1989 Properties of Ginzburg–Landau attractors associated with their Lyapunov vectors and spectra. *Phys. Lett.* A **140**, 317.

KEEFE, L., MOIN, P. & KIM, J. 1989 Applications of chaos theory to shear turbulence. *NASA Ames Res. Center, preprint* MS202A-1.

KOLMOGOROV, A. N. 1960 In Seminar Notes edited by Arnold, V. I. & Meshalkin, L. D., *Usp. Mat. Nauk* **15**, 247.

KRAICHNAN, R. H. 1967 Inertial ranges in two- and three-dimensional turbulence. *Phys. Fluids* **10**, 1417.

KRAICHNAN, R. H. 1987 Reduced descriptions of hydrodynamic turbulence. *J. Statist. Phys.* **51**, 949.

LAFON, A. 1985 Etude des attracteurs pour des écoulements bidimensionnels de fluides visqueux incompressibles. Thèse d'Etat Université Paris 6.

LANDAU, L. D. & LIFSHITZ, E. M. 1971 *Mécanique des Fluides*, chap. 3, p. 154. Moscow: Mir.

LEGRAS, B., SANTANGELO, P. & BENZI, R. 1988 High resolution numerical experiments for forced two-dimensional turbulence. *Europhys. Lett.* **5**, 37.

MANNEVILLE, P. 1985 Lyapunov exponents for the Kuramoto–Sivashinsky model. In *Macroscopic Modeling of Turbulent Flows* (ed. U. Frisch, J. B. Keller, G. Papanicolaou, O. Pironneau). Springer.

MESHALKIN, L. D. & SINAÏ, Y. A. & YA, G. 1961 *Z. Angew. Math. Mech.* **25**, 1700.

OBUKHOV, A. M. 1983 *Russ. Math. Survey* **38**, 113.

OHKITANI, K. & YAMADA, M. 1989 *Prog. Theor. Phys.* **81**, 329.

OSELEDEC, V. I. 1968 A multiplicative ergodic theorem. Lyapunov characteristic numbers for dynamical systems. *Trans. Moscow Maths Soc.* **19**, 197.

SHE, Z. S. 1987 Metastability and vortex pairing in the Kolmogorov flow. *Phys. Lett.* A **124**, 161.

YAMADA, M. & OHKITANI, K. 1988 Lyapunov spectrum of a model of two-dimensional turbulence. *Phys. Rev. Lett.* **60**, 983.